NASA

Technical Memorandum 78066

Stratospheric Sounding by Infrared Heterodyne Spectroscopy

Mian M. Abbas, Virgil G. Kunde, Michael J. Mumma, Theodor Kostiuk, David Buhl and Margaret A. Frerking

JANUARY 1978

National Aeronautics and Space Administration

Goddard Space Flight Center
Greenbelt, Maryland 20771

STRATOSPHERIC SOUNDING BY INFRARED HETERODYNE SPECTROSCOPY

Mian M. Abbas*
Department of Physics and Astronomy
University of Maryland, College Park, MD 20742

Virgil G. Kunde, Michael J. Mumma,
Theodor Kostiuk and David Buhl
NASA/Goddard Space Flight Center
Infrared and Radio Astronomy Branch, Code 693
Greenbelt, MD 20771

and

Margaret A. Frerking**
Department of Physics and Research
Laboratory of Electronics
Massachusetts Institute of Technology
Cambridge, MA 02139

*Mail Address: Infrared and Radio Astronomy Br., Code 693
NASA/Goddard Space Flight Center
Greenbelt, MD 20771

**Present Address: Bell Telephone Laboratories
Crawford Corner Road
Holmdel, N.J. 07733

ABSTRACT

Intensity profiles of infrared spectral lines of stratospheric constituents can be fully resolved with a heterodyne spectrometer of sufficiently high resolution ($\sim$ 5 MHz or 0.000167 cm^{-1}). The constituents' vertical distributions can then be evaluated accurately by analytic inversion of the measured line profiles.

Estimates of the detection sensitivity of a heterodyne receiver are given in terms of minimum detectable volume mixing ratios of stratospheric constituents, indicating a large number of minor constituents which can be studied. Stratospheric spectral line shapes, and the resolution required to measure them are discussed in light of calculated synthetic line profiles for some stratospheric molecules in a model atmosphere. The inversion technique for evaluation of gas concentration profiles is briefly described and applications to synthetic lines of O_3, CO_2, CH_4 and N_2O are given. Some recent heterodyne measurements of CO_2 and O_3 absorption lines are analytically inverted and the vertical distributions of the two gases are determined.

1. Introduction

Stratospheric trace constituents may be detected through measurements of their infrared vibrational-rotational lines, and absolute column abundances can be determined from the measured line equivalent widths. If the individual line shapes are also measured, an inverse solution of the radiative transfer equation may be found which yields the density-altitude profile (for transient species) or the temperature-altitude profile (for a uniformly mixed gas). Measurements of individual line intensity profiles are very difficult by conventional spectroscopic methods, particularly when the gas is distributed throughout atmospheric regions having widely different total pressures. The line profiles will then consist of pressure broadened wings and doppler cores, imposing severe restrictions on the spectral resolution needed to fully resolve the line. Infrared heterodyne spectroscopy (IRHS) is well suited to atmospheric studies because of its high specific detection sensitivity and its ultrahigh spectral resolution ($\sim$ 5 MHz = .00017 cm^{-1}). At this resolution, individual line shapes can be measured without significant instrumental distortion and the analysis may be carried out in a straightforward manner.

Application of heterodyne spectroscopy to stratospheric studies is still in its developing stages, and only preliminary attempts at measurements and some feasibility studies have been made (Seals and Peyton, 1975; Seals, 1974; Peyton et al. 1977; Menzies and Seals, 1977). The purpose of this paper is to present additional calculations on the

feasibility of IRHS stratospheric composition measurements, and to report preliminary measurements and analyses of CO_2 and O_3 absorption lines measured with ground-based IRHS systems.

Stratospheric measurements may be carried out either in absorption (observing the sun or the moon), or in self-emission (observing atmospheric emission lines directly). Absorption measurements are intrinsically absolute and the precision is limited by the signal-to-noise ratio (SNR) achieved. For solar measurements, the SNR may be as high as ~100,000, depending upon the volume mixing ratio of the gas, the strength of the line, the integration time, and the spectral bandwidth chosen. Lines with optical depths as small as 10^{-5} can be measured in this mode. The expected SNR's for self-emission are much lower, thus species investigated in this mode are limited to those having nearly optically thick infrared lines.

This paper is limited in scope to ground-based solar-absorption measurements. The basic theory employed in making the radiative transfer calculations is discussed in section 2. Section 3 deals with the feasibility and application of an IRHS for stratospheric measurements, treating the detection sensitivity, minimum detectable volume mixing ratios of stratospheric constituents, and line shapes of infrared absorption lines in the stratosphere. The method of infrared spectral line inversion is briefly discussed in Section 4. Results of solar-absorption measurements and analyses of CO_2 and O_3 lines made with CO_2 - laser and tunable-diode-laser heterodyne spectrometers are given in Section 5.

2. Theoretical Considerations

The downward spectral intensity, corresponding to a ground-based observation of the sun, may be written as

$$I_\nu = B_\nu(T_\odot)\ \tau_\nu^s + \int_{\tau_\nu^s}^{1} B_\nu(T)\ d\tau_\nu(P,T), \tag{1}$$

where B_ν is the Planck function at temperature T, $T_\odot$ is the solar brightness temperature (K), P is atmospheric pressure (atm), τ_ν is the transmittance at frequency ν from the atmospheric layer to the observer, and τ_ν^s is the transmittance from the top of the atmosphere to the ground The atmospheric transmittance τ_ν is

$$\tau_\nu = \exp\left[-\int \sum_i k_{\nu_i}\ du_i\right], \tag{2}$$

where k_{ν_i} is the specific absorption coefficient (cm^{-1}-atm^{-1}) at frequency ν for the ith species, and the summation extends over all absorbing species. The element of column density (cm-atm) is

$$du_i(P) = q_i^v(P)\left(\frac{P}{P_{NTP}}\right)\left(\frac{T_{NTP}}{T}\right) ds = q_i^v\left(\frac{P}{P_{NTP}}\right)\left(\frac{T_{NTP}}{T}\right) \sec\theta_z\ dz, \tag{3}$$

where $q_i^v(P)$ is the volume mixing ratio for the ith species, and θ_z is the zenith angle at level z. NTP denotes normal temperature and pressure. θ_z is related to the starting parameters at height H1 by

$$\sec\theta_z = \frac{n_z(R_o + z)}{\left[n_z^2(R_o + z)^2 - (R_o + H1)^2 \sin^2\theta_{H1}\, n_{H1}^2\right]^{1/2}}, \tag{4}$$

where the refractive indices n_{H1} and n_z refer to the values at the levels H1 and z. The geometry of the ray path for solar observations is shown in Fig. 1. The ray tracing technique used is similar to that

described by Selby and McClatchey (1972), Snider (1975) and Goldman and Snider (1975).

The element of column density (du) may also be written in terms of the mass mixing ratio

$$du = \frac{1}{g}\, q_i(P) \sec\theta\, dP, \tag{5}$$

where $q_i(P) = q_i^v(P)\ {}^{m_i}/_{m_T}$ with the masses referring to the species (i) and to the average molecular mass of the gas. The absorption coefficient at frequency ν for species i is obtained by summing the contributions from all lines

$$k_\nu = \Sigma_\ell k_{\nu\ell}\ (P,T)\ , \tag{6}$$

where the absorption coefficient for an individual line may be written

$$k_{\nu\ell}(P,T) = b \int k_{\nu\ell}\, d\nu = S_\ell(T)\ b(P,T)\ , \tag{7}$$

where S_ℓ is the integrated line intensity in cm^{-1} $(cm\ atm)^{-1}$ and b is the line shape function.

A convenient technique for calculating the absorption coefficients for an individual line is based on separating the contribution from each line into a wing contribution and a direct contribution near the line center ($\nu \leq \nu_c \pm \delta$), where δ is model dependent and in the present case is chosen to be 3.5 cm^{-1} (Kunde and Maguire, 1974). The wing contribution is calculated by assuming a Lorentzian line shape, and the direct contribution by using the mixed Doppler-Lorentz line shape (Voigt line shape) formula for which the function b is

$$b(P,T) = \frac{1}{\alpha_D}\left(\frac{\ell n 2}{\pi}\right)^{1/2} \frac{y}{\pi} \int_{-\infty}^{\infty} \frac{e^{-t^2}}{y^2 + (x-t)^2}\, dt\ , \tag{8}$$

with

$$y = \frac{\alpha_L}{\alpha_D} (\ln 2)^{1/2} , \tag{9}$$

and

$$x = \frac{(\nu - \nu_o)}{\alpha_D} (\ln 2)^{1/2} , \tag{10}$$

where α_L and α_D are the half-width at half-maximum of Lorentz and Doppler broadened lines and

$$\alpha_D = 3.58 \times 10^{-7} \nu \left(\frac{T}{M}\right)^{1/2} \text{ cm}^{-1} . \tag{11}$$

The line centers, line strengths, and half-widths employed in this paper for O_3, N_2O and H_2O are taken from the AFCRL molecular line parameter atlas (McClatchey et al, 1973), while the CO_2 and CH_4 line parameters have been generated with a quantum mechanical model (Maguire, 1977). The dependence of line strength on temperature T is given by

$$S(T) = \frac{S_o(T_o)\, Q_v(T_o)\, Q_r(T_o)}{Q_v(T)\, Q_r(T)} \exp\{1.439\, E''[(T-T_o)/T\, T_o]\}, \tag{12}$$

where S_o is the line strength at the reference temperature T_o (296 °K), E" is the lower state energy (cm^{-1}) of the transition, and Q_v and Q_r are the vibrational and rotational partition functions. The basic equations and the methods outlined here are employed in calculating spectra of atmospheric gases as discussed in the following sections.

3. Feasibility of IRHS Stratospheric Measurements

A plot of representative constituent mixing ratio profiles is shown in Fig. 2, and a list of some selected molecules having transitions in the 10μm terrestrial window is given in Table I. An overview of

the observed atmospheric spectrum (0.25 cm^{-1} resolution) is given in Fig. 3 (Kunde et al. 1977).

(a) Sensitivity of a Heterodyne Spectrometer

In a heterodyne receiver, the infrared signal from the source is mixed with coherent radiation from a local oscillator (such as a CO_2 laser or a tunable diode laser) and the difference frequency signal is detected by radio frequency techniques. The basic theory and sensitivity considerations of heterodyne spectroscopy have been given in the literature. (e.g., Teich, 1971; Abbas, et al. 1976). Here, we consider its sensitivity for detection of stratospheric molecules.

The SNR of a heterodyne receiver is

$$\frac{S}{N} = \frac{P^s}{\Delta h\nu} \left(\frac{\tau}{B}\right)^{1/2} , \tag{13}$$

where Δ is the total system degradation from the ideal quantum detection limit, τ is the integration time, B is the bandwidth of a single resolving element of the system, and P_s is the source power contained in the bandwidth and the etendue ($A\Omega \sim \lambda^2$) of a heterodyne receiver. Equation (13) yields an expression for the noise-equivalent radiance of a heterodyne receiver as:

$$(NER)_{Het} = \frac{\Delta hc}{\lambda^3 (B\tau)^{1/2}} \quad (W\ cm^{-2}\ Sr^{-1}\ Hz^{-1}) . \tag{14}$$

Equation (14) indicates that the sensitivity of a heterodyne receiver

improves rapidly with longer wavelength, varying as λ^{-3}. In principle, the spectral bandwidth (B) may be decreased arbitrarily for increasingly higher resolution, but only at the expense of a corresponding decrease in sensitivity.

We now estimate the minimum detectable column density and volume mixing ratio. We assume a homogeneous isothermal atmosphere at temperature T with uniform volume mixing ratio q_i^v and source surface temperature $T_\odot$. Equations (1) and (2) then give an expression for the minimum detectable vertical column density for the solar absorption mode

$$u_{min} = \frac{(NER)_{Het}}{k_\nu(T,P)\ B_\nu(T_\odot)\ \sec\theta} . \tag{15}$$

The minimum detectable volume mixing ratio then becomes

$$q^v_{min} = \frac{(NER)_{Het}}{k_\nu(T,P)\ B_\nu(T_\odot)\ u_T\ \sec\theta} . \tag{16}$$

where u_T is the total vertical column density and $T_\odot$ is the solar brightness temperature.

For a moderately strong atmospheric line ($S \sim 1$ cm^{-1} (cm-atm^{-1}), $k \sim 50$ (cm-atm)$^{-1}$ and for instrumental parameters of B = 5 MHz, τ = 1000 sec, Δ = 30, sec θ = 1, the noise equivalent radiance and minimum detectable volume mixing ratio are

$$(NER)_{Het} \sim 8 \times 10^{-18}\ (\text{W cm}^{-2}\ \text{Sr}^{-1}\ \text{Hz}^{-1}) \tag{17}$$

and

$$q^v_{min} \sim 2 \times 10^{-12} \text{ or } 2 \text{ pptv} \tag{18}$$

This detection limit has been derived only for obtaining an order of magnitude estimate of the sensitivity of an IRHS.

Fig. 2 indicates that at this sensitivity almost all of the important stratospheric constituents may be detected with a heterodyne spectrometer. Note that while Eq. (18) is based on a path length of one air-mass, slant paths at balloon altitudes can increase this to ~ 20 air-masses with a concomitant increase in sensitivity.

(b) Measurements of Stratospheric Absorption Lines

The calculated transmittances for the mid-latitude summer model atmosphere of Selby and McClatchey (1972) and the volume mixing ratios of Fig. 2 are given in Figs. 3-6. The computed spectra exhibit absorption lines of CO_2, O_3, CH_4 and N_2O. The water vapor concentration of the model atmosphere was modified to yield a total vertical column density of 682 cm-atm, corresponding to field conditions during the observations discussed in section 5.

An important consideration in the measurement of line profiles and in the subsequent retrieval of information is the type of lineshape involved. The widths are on the order of 1 GHz with narrow cores. The widths of moderately strong lines of primarily stratospheric molecules (e.g. O_3, CO) are on the order of a few hundred MHz. Representative lineshapes have been computed for stratospheric (z = 45 km) and tropospheric (z = 12 km and z = 0 km) levels for the 940.55 cm^{-1} (P24) line of the 961 cm^{-1} CO_2 band and are shown in Fig. 7. At 45 km the doppler half-width is ~ 8 x 10^{-4} cm^{-1} (24 MHz) and the core of the line is essentially shaped by doppler broadening. For $\Delta\nu$ greater than ~1.6 x 10^{-3} cm^{-1} (50 MHz) the lineshape is dominated by pressure

broadening. At the z = 12 and 0 km levels the entire line is shaped by pressure broadening effects. Measurements of doppler cores (formed in the stratosphere) thus require high spectral resolution (~ 5 MHz) whereas lower resolution (~50 MHz) will be sufficient in the wings (formed in the troposphere).

4. Inversion of Infrared Spectral Lines

Atmospheric parameters may be extracted by analysis of individual spectral lines measured at sufficiently high spectral resolution through an inverse solution of the radiative transfer equation (1). The inversion of an appropriately chosen line can provide constituent concentration profiles in both the stratosphere and the troposphere.

Atmospheric self-emission in Eqn. (1) usually may be ignored for solar observations, and the observed intensity can be written as

$$I_\nu^{ob} = B_\nu(T_\odot)\ \tau_\nu^{ob}. \tag{19}$$

The observed transmittance (τ_ν^{ob}) then is:

$$\tau_\nu^{ob} = I_\nu^{ob}/B_\nu(T_\odot). \tag{20}$$

Combining Eqs. (2) and (5), the atmospheric transmittance may be written in the form

$$\ln \tau_\nu^s = \frac{1}{g}\int_0^P \Sigma_i\ k_{\nu i}\ (T,P)\ q_i(P)\ dP. \tag{21}$$

Equation (21) suggests that the mixing ratios of the absorbing gas may be iteratively evaluated, with k_ν used as a weighting function. The iterative scheme used here is similar to that described in the literature (Seals, 1974; Smith, 1970; Menzies and Chahine, 1974).

The plots of weighting functions (normalized absorption coefficients) for some absorption lines of O_3, CH_4 and N_2O are shown in Figs. (8)-(10). The weighting functions for O_3 in the 9.4μm band reach peaks upto heights of $\sim$ 30-35 km for ground-based observations. The weighting functions reach peaks upto ~25 km for CH_4 and N_2O absorption lines in the 1230 cm^{-1} to 1250 cm^{-1} range. The altitudes which may be probed by this method are determined by the shapes and the levels at which the weighting functions (k_ν) reach their peaks. At altitudes where pressure broadening is dominant, the Voight profile reduces to a Lorentzian and

$$k_\nu(P) = \frac{1}{\pi} \frac{S(T)\,\alpha(P,T)}{(\nu-\nu_o)^2 + \alpha^2(P,T)} \quad . \tag{22}$$

Setting the derivative of $k_\nu(P)$ with respect to $\alpha(P,T)$ equal to zero and solving for $\alpha(P)$, indicates that for transitions with small values of lower state energy E" (so that the dependence of line strength on T may be ignored), $k_\nu(P)$ is maximum at levels where $\alpha(P,T) \sim (\nu-\nu_o)$. At altitudes where doppler broadening is predominant ($\geq$ 35 km), k_ν increases monotonically and thus cannot be used as a weighting function. The inversion technique discussed here is thus useful only for altitudes at which the lines are pressure broadened. A different mode of observation and inversion technique has to be employed for probing higher regions.

Inversion of a specific line is carried out in the following way. The atmosphere is divided into N layers (35 in the present work). The vertical temperature profile T(z) is assumed or evaluated by analyzing the absorption line of a well mixed gas such as CO_2 (T(z) need not be known as accurately for solar absorption measurements as

for the self-emission mode). An initial guess for the mixing ratio profile $q_i^{j,m}$ is made (j denotes the level and m the iteration). The absorption coefficients and transmittances $k_{\nu_k}^{j,m}$ and $\tau_{\nu_k}^{m}$ for an appropriately chosen set of frequencies ν_k are calculated monochromatically by summing the contributions of individual molecular absorption lines as discussed in section 2. An improved mixing ratio profile $q_i^{j,m+1}$ is then estimated at the levels corresponding to the peaks of the weighting functions from

$$q_i^{j,m+1} = q_i^{j,m} \left(\ell n\, \tau_\nu^{ob} / \ell n\, \tau_\nu^{m}\right) \tag{23}$$

The complete profile is interpolated from the corrected values and the iterative process is continued until the calculated τ_ν^m converge to the observed values of τ_ν^{ob} over the entire set of chosen frequencies in a least squares sense. The process is stopped when the RMS residual is of the same order as the noise level of the measurements.

The weighting functions are chosen such that a sufficient number of levels are included for interpolation of the gas mixing ratio profile. The vertical resolution of the retrieved profile is then dependent on the shapes of the weighting functions, which are determined by the line strength and the lower state energy of the transition. If the weighting functions are sharply peaked, the inversion procedure converges in 15-20 iterations.

The mixing ratio profiles retrieved by inverting synthetic (O_3, CH_4, N_2O) and measured (CO_2) absorption lines (Figs. 4-6,14) are shown in Figs. 11 and 12. The initial guess profiles and the model profiles

are also shown. These results demonstrate the internal consistency of the method, and indicate that inversion of infrared absorption lines measured with sufficiently high spectral resolution can lead to vertical concentration profiles of stratospheric constituents to heights ~ 30 km with vertical resolution ~ 4 km.

5. Atmospheric Absorption Measurements

The atmospheric absorption measurements reported here are based on solar observations of absorption lines of CO_2 and O_3 in the 10μm band. The measurements were made with a CO_2-laser heterodyne spectrometer at Goddard Space Flight Center, and a tunable diode-laser heterodyne spectrometer at MIT.

A schematic of the Goddard CO_2-laser spectrometer is shown in Fig. 13. This system (Mumma, et al. 1977), presently interfaced with a 48" telescope at the optical test site in Greenbelt, MD., employs a CO_2 laser as local oscillator, a HgCdTe photodiode as a mixer, and two sets of IF filter banks. The high resolution filter bank consists of 40 sequential filters of 5 MHz resolution covering a total of 200 MHz bandwidth. The low resolution filter bank has 23 filters of 50 MHz resolution with a total bandwidth of 1 GHz and one filter of 1 GHz bandwidth. The CO_2 laser is grating tunable from line to line, so that the detection of atmospheric lines is limited to those which lie within $\pm$ 1.5 GHz of a CO_2 laser line. This restriction requires knowledge of the line center frequencies of the transitions to be observed.

Fig. 14 shows the observed profile of an atmospheric CO_2 line (ν_o = 967.7072 cm^{-1}) measured on Feb. 10, 1977 with the low resolution filter bank. The Doppler broadened core, formed at high altitudes, can be identified. This line was inverted and the retrieved mixing ratio profile for CO_2 is shown in Fig. 12. The computed absorption line based on the retrieved mixing ratio profile is shown by the solid curve in Fig. 14. The retrieved profile shows that CO_2 is well mixed to at least 50 km, in agreement with independent results. (e.g. Reiter et al., 1975).

Fig. 15 shows an O_3 absorption line (ν_o = 1044.9787 cm^{-1} near the CO_2 - P(22) line in the 19.4μm band) measured on April 8, 1977 at various values of air-mass (sec θ). The high and low resolution spectra are shown on the left and right hand sides respectively. With increasing air-mass, decreasing intensities and increasing line saturation are evident in both spectra. These measurements are of a preliminary nature. This line, with lower state energy of 707.21 cm^{-1} and line strength S = 0.011 cm^{-1} $(cm\text{-}atm)^{-1}$ is not well suited for inversion. However, a measurement of this absorption line profile as a function of air-mass, indicates the capability of IRHS for investigating the daytime variation of O_3 concentration in the stratosphere. The nightime variations may be measured by making similar observations of the moon.

Atmospheric solar absorption measurements were made with a tunable diode-laser spectrometer in Cambridge, MA., on Jan 2, 1977 around noon with the solar zenith angle between 67° to 64°. The air temperature was ~ 272 °K with relative humidity ~ 50%.

A detailed description of the tunable diode laser spectrometer and preliminary results have been given elsewhere (Frerking and Muehlner, 1977). The spectrometer employed a liquid nitrogen cooled PbSnSe diode laser as a local oscillator and a HgCdTe photodiode as a mixer. The diode laser was continuously tunable over the spectral range of 1010.9 to 1011.8 cm^{-1}. The total bandwidth (2B) of the IF filters used in these measurements could be chosen as 200 MHz or 70 MHz, providing spectral resolutions of 0.0067 cm^{-1} or 0.0023 cm^{-1} respectively.

The atmospheric spectrum taken with a spectral resolution of 0.0023 cm^{-1} on Jan. 2, 1977, shows absorption lines of O_3 in the spectral range of 1010.9 to 1011.8 cm^{-1} (Fig. 16). The spectral data on the eight O_3 lines identified in Fig. 16b are given in Table II. Since the atmospheric transmittance was not directly calibrated, an absolute transmittance scale was established by normalizing to the value at 1011.2 cm^{-1} calculated from a mid-latitude model atmosphere with a total water vapor content of 625 cm-atm (precipitable water = 0.50 cm). This water content corresponds to local conditions at the time of observations (Radiosonde data, National Weather Service).

The strong ozone lines with $S \sim 0.3$ (in cm-atm units) are saturated (Fig. 16b). The saturation is particularly strong because the air-mass during the measurements was ~ 2.3 (solar zenith angle 65°) even though the measurements were made around noon. The saturation results in a loss of spectral information from the upper stratosphere, since the weighting functions for frequencies near line center peak

at heights ~ 25-35 km. A line of moderate intensity has to be used to probe the upper stratosphere from the ground. In addition, transitions with smaller values of LS energy are needed to reduce the temperature dependence. A comparison of the numerical values of S and LS energy listed in Table III, shows that lines 3,4, and 8 are most suitable for analysis. Lines 4 and 8 are saturated, but line 3 with a lower value of S, may be used in conjunction with line 4 or 8 for analysis. The weaker lines such as 1 or 2, with larger LS values, have weighting functions which do not have sharp peaks and are thus not suitable for inversion.

Lines 3 and 8, with line centers at ν_o = 1011.1039 cm^{-1} and ν_o = 1011.6636 cm^{-1} respectively, are shown at high resolution in Fig. 17a,b. The retrieved mixing ratio profile of O_3 obtained through an inversion of these two lines is shown in Fig. 18. Because of saturation of the two lines and insufficient resolution near the line center, the retrieved O_3 profile is accurate up to heights of about 25-28 km only. A fixed value of $q^v = 2.9 \times 10^{-6}$ is assumed at a height of 50 km and the complete vertical profile is then interpolated. The retrieved profile corresponds to a total vertical O_3 column density ~0.37 cm atm. This value compares with a column density of 0.398 cm-atm of the mid-latitude model O_3 profile shown in Fig. 18.

The computed transmittances for the two lines based on the retrieved O_3 profile agree well with the observed values (Fig. 17). The synthetic spectrum was calculated over the spectral range

1019.9-1011.8 cm^{-1} from the retrieved ozone profile (Fig. 16c). The line parameters such as line centers, line strengths and lower state energies were taken from the AFCRL line parameter atlas (McClatchey et al., 1973). The half-width for ozone used was 0.07 cm^{-1} at NTP. No attempt has been made to correct the line centers in the synthetic spectrum to conform with the observed positions.

A comparison between the observed and synthetic spectra (Figs. 16b and 16c) shows that there are significant differences, indicated by missing or extra lines. No attempt has been made to achieve a closer match between the two plots, but the differences are very likely due to inaccuracies in line parameters used in generating the synthetic spectrum. Existing uncertainties in the line centers and intensities are evident when comparing ν_3 line parameters of Barbe et al (1977), Menzies (1976), and the AFCRL atlas (McClatchey et al., 1973). Extra lines could also be due to other gases.

Conclusions:

The measurements and analyses presented in this paper indicate the usefulness of heterodyne measurements in the infrared for detection of a large number of stratospheric constituents. The vertical mixing ratio profiles and the total abundances of some constituents may be determined with high vertical resolution ($\sim$ 4 km) and the diurnal variation may be followed by tracking the sun or the moon. Interpretation of heterodyne measurements and the accuracy of analysis is limited by the availability of accurate line parameters. A parallel program

of accurate laboratory measurements of line parameters, is essential for identification and analysis of stratospheric constituents. Precision line frequency measurements permit extraction of wind velocities in some cases. With the availability of tunable diode lasers covering the entire 10μm window, heterodyne measurements are expected to play a prominent role in stratospheric research.

Acknowledgement

We thank Gary Burgess for the extensive help in carrying out the numerical computations presented in this paper. The contributions of other members of the Infrared Heterodyne Group at Goddard Space Flight Center are gratefully acknowledged.

REFERENCES

Abbas, M. M., M. J. Mumma, T. Kostiuk, and D. Buhl, Applied Optics, 15, 427-436, 1976.

Barbe, A., C. Secroun, P. Jouve, N. Monnanteuil, J. C. Depannemaeker, B. Duterage, J. Bellet, and P. Penson, J. of Molecular Spectroscopy, 64, 343-364, 1977.

Frerking, M. A., and D. J. Muehlner, Applied Optics, 16, 526-528, 1977.

Kunde, V. G., and W. C. Maguire, J. Quant. Spectrosc. Radiat. Transfer, Vol. 14, 803-817, 1974.

Kunde, V. G., R. A. Hanel, and L. W. Herath, Icarus, 32, 210-224, 1977.

Maguire, W. C., Private communication.

Menzier, R. T., and M. T. Chahine, Applied Optics, No. 13, 2840-2849, 1974.

Menzies, R. T., Applied Optics, 15, 2597-2599, 1976.

Menzies, R. T., and R. K. Seals, Jr., preprint, 1977.

Mumma, M. J., T. Kostiuk, and D. Buhl, Optical Engineering, 17, 1977.

McClatchey, R. A., W. S. Benedict, S. A. Clough, D. E. Burch, R. F. Calfee, K. Fox, L. S. Rothman, and J. S. Garing, ARCRL-TR-73-0096, 1973.

Peyton, B. J., J. Hoell, R. A. Lange, R. K. Seals, Jr., M. G. Savage, and F. Allario, Preprint, 1977.

Reiter, E.R., E. Bauer, and S.C. Coroniti, ed., The Natural Stratospheres of 1974, CIAP Monograph DOT-TST-75-51, 1975.

Seals, R. K., AIAA Journal, 12, No. 8, 1118-1122, 1974.

Seals, R. K., and B. J. Peyton, Proc. Intr. Conf. on Environ. Sensing and Assesment, Vol. 1, p.1-7, 1975.

Selby, J. E. A., R. M. McClatchey, Tech. Rept. ARCRL-82-0745, Environ. Res. Pa. No. 427, 1972.

Smith, W. L., Applied Optics. Vol. 9, No. 9, 1993-1999, 1970.

Snider, D. E., and A. Goldman, Ballistic Res. Labs. Report No. 1790, 1975.

Snider, D. E., J. Atm. Sci., 32, 2178-2184, 1975.

Teich, M. C., in Infrared Detectors: Semiconductors and Semimetals (Academic, New York, 1971) Vol. 5, p.361.

List of Tables

Table I. Some Selected Gases with Transitions In the Intermediate Infrared

Gas	Accessible Spectral Region (cm^{-1})		
O_3	1000-1100	*	
NO_x:			
N_2O	1190,1290	*	(Hot Bands)
NO_2	1621		
HNO_3	890		
N_2O_5	1000		
HO_x:			
H_2O	900-1200		
HO_2	1101,1390		
H_2O_2	880,1266,1380		
Cl:			
CCl_4	768,789		
$CFCl_3$ (Freon 11)	847		
CF_2Cl_2 (Freon 12)	920-930	*	
CH_3Cl	732,1355	*	
ClO	850	*	
$ClONO_2$	780,1490		
Br:			
CH_3Br	954,1443		
BrO	853,1483		
NH_3	930-970		
CH_4	1306		
CH_3F	1047	*	

*Line data known accurately for at least some lines.

Table II. Spectral data for the ozone absorption lines in Fig. 16b

Line No.	ν_o cm^{-1}	S cm^{-1} $(cm\ atm)^{-1}$	LS Lower State Energy cm^{-1}	Quantum Numbers Upper State (J', K_a', K_c')	Quantum Numbers Lower State (J'', K_a'', K_c'')
1	1011.0345	0.0769	649.20	24, 11, 14	25, 11, 15
2	1011.0625	0.0277	768.90	10, 2, 9	11, 2, 10
3	1011.1039	0.197	540.84	27, 8, 19	28, 8, 20
4	1011.2959	0.374	442.06	29, 4, 25	30, 4, 26
5	1011.3232	0.157	570.05	26, 9, 18	27, 9, 19
6	1011.3579	0.118	606.21	22, 14, 9	23, 14, 10
7	1011.4202	0.293	478.21	28, 6, 23	29, 6, 24
8	1011.6636	0.414	422.96	29, 3, 26	30, 3, 27

LIST OF FIGURES

(6) 0.00333 (7) 0.00500 (8) 0.0067 (9) 0.00833 (10) 0.01000

(11) 0.01167

Fig. 9. Weighting function for the CH_4 line of Fig. 5 with line center ν_o = 1228.8800 cm^{-1}, for frequencies with $\Delta\nu$ (cm^{-1}) given by:

(1) 0.00500 (2) 0.00583 (3) 0.00750 (4) 0.00917 (5) 0.01000

(6) 0.01333 (7) 0.01833 (8) 0.02233 (9) 0.02667 (10) 0.03333.

Fig. 10 Weighting function for the N_2O line of Fig. 6 with line center ν_o = 1252.5600 cm^{-1}, for frequencies with $\Delta\nu$ (cm^{-1}) given by:

(1) 0.00267 (2) 0.00333 (3) 0.00417 (4) 0.00500 (5) 0.00583

(6) 0.00833 (7) 0.01167 (8) 0.01333 (9) 0.01667 (10) 0.01833

(11) 0.02167 (12) 0.02667 (13) 0.03333.

Fig. 11 The retrieved volume mixing ratio profile of atmospheric ozone, based on an inversion of the synthetic line shown in Fig. 4. The initial guess and the nominal model profile are also shown.

Fig. 12 The retrieved volume mixing ratio profiles of atmospheric N_2O, CH_4 and CO_2 based on lines shown in Figs. 6,5,14. The initial guess and nominal model profiles are also shown. The retrieved CO_2 profile shown is obtained from an inversion of the measured atmospheric CO_2 absorption line of Fig. 14.

Fig. 13 A schematic of the infrared heterodyne spectrometer at Goddard Space Flight Center. The source signal is mixed

with radiation from a local oscillator at the HgCdTe photomixer. The 0-1.5 GHz intermediate frequency (IF) signal is then fed into the RF filter bank. The outputs of the 64 filters are separately multiplexed, integrated, and synchronously detected in the calculator. A magnetic tape unit, a graphics data terminal and a line printer, enable storage display and retrieval of the output.

Fig. 14 Atmospheric CO_2 R(8) absorption line measured at 50 MHz resolution.

Fig. 15 Atmospheric O_3 absorption lines observed in solar-absorption mode as a function of air mass.

Fig. 16 Atmospheric ozone absorption spectra taken with tunable diode-laser heterodyne spectrometer with a spectral resolution of 0.0023 cm^{-1}. (a) A single scan (b) An average of five scan (c) Synthetic spectrum based on the retrieved O_3 mixing ratio profile of Fig. 18.

Fig. 17a,b Smoothed high resolution plots of the two O_3 absorption lines (#3 and #8 Fig. 16b). The synthetic lines based on the retrieved O_3 mixing ratio profile of Fig. 18 are shown with dashed lines.

Fig. 18. The retrieved volume mixing ratio profile of ozone obtained from inversion of the two observed lines in Fig. 17. The nominal model profile is shown with the dashed line.

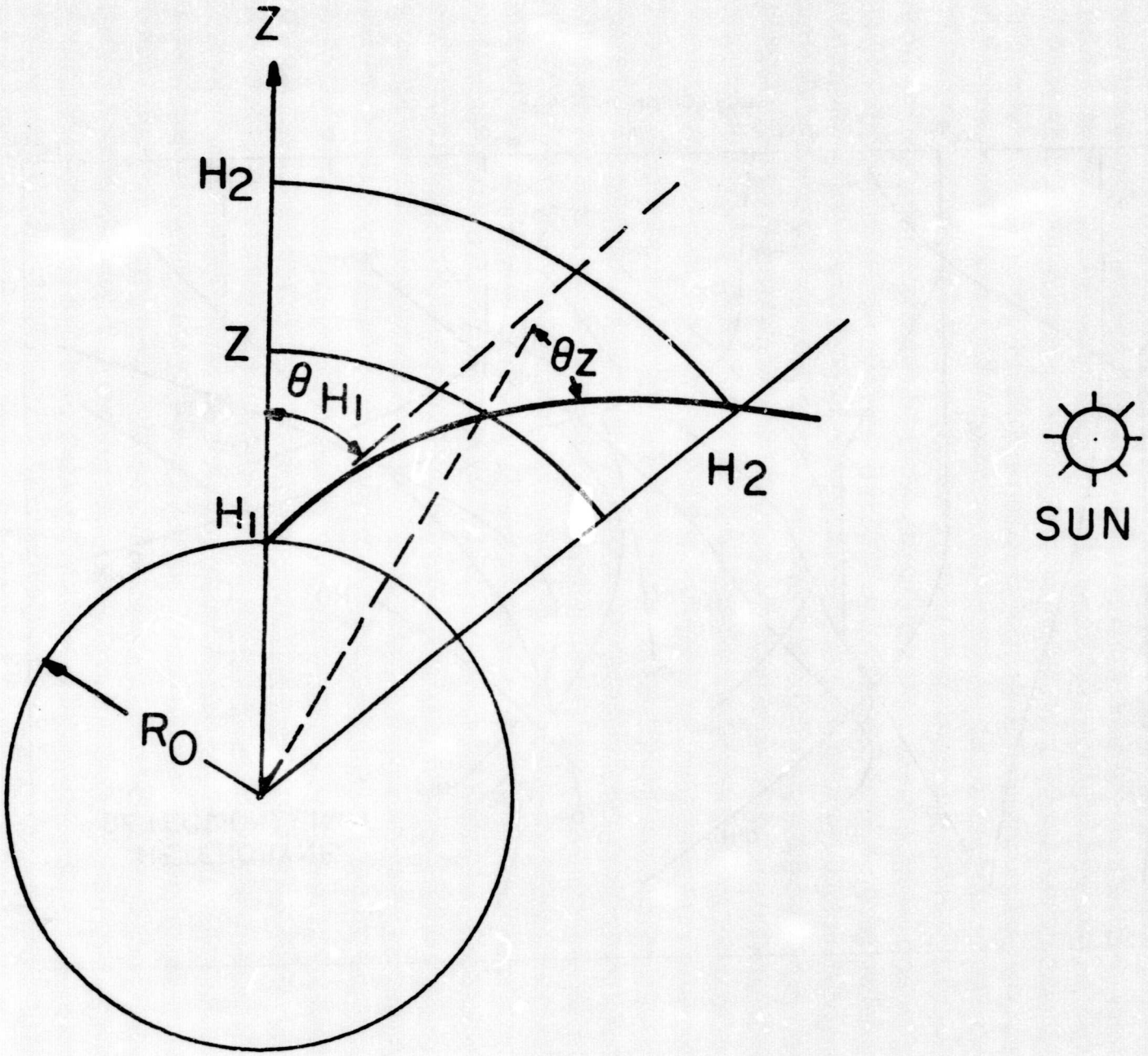
Z
H2
Z
θ H1
θz
H2
H1
RO
SUN

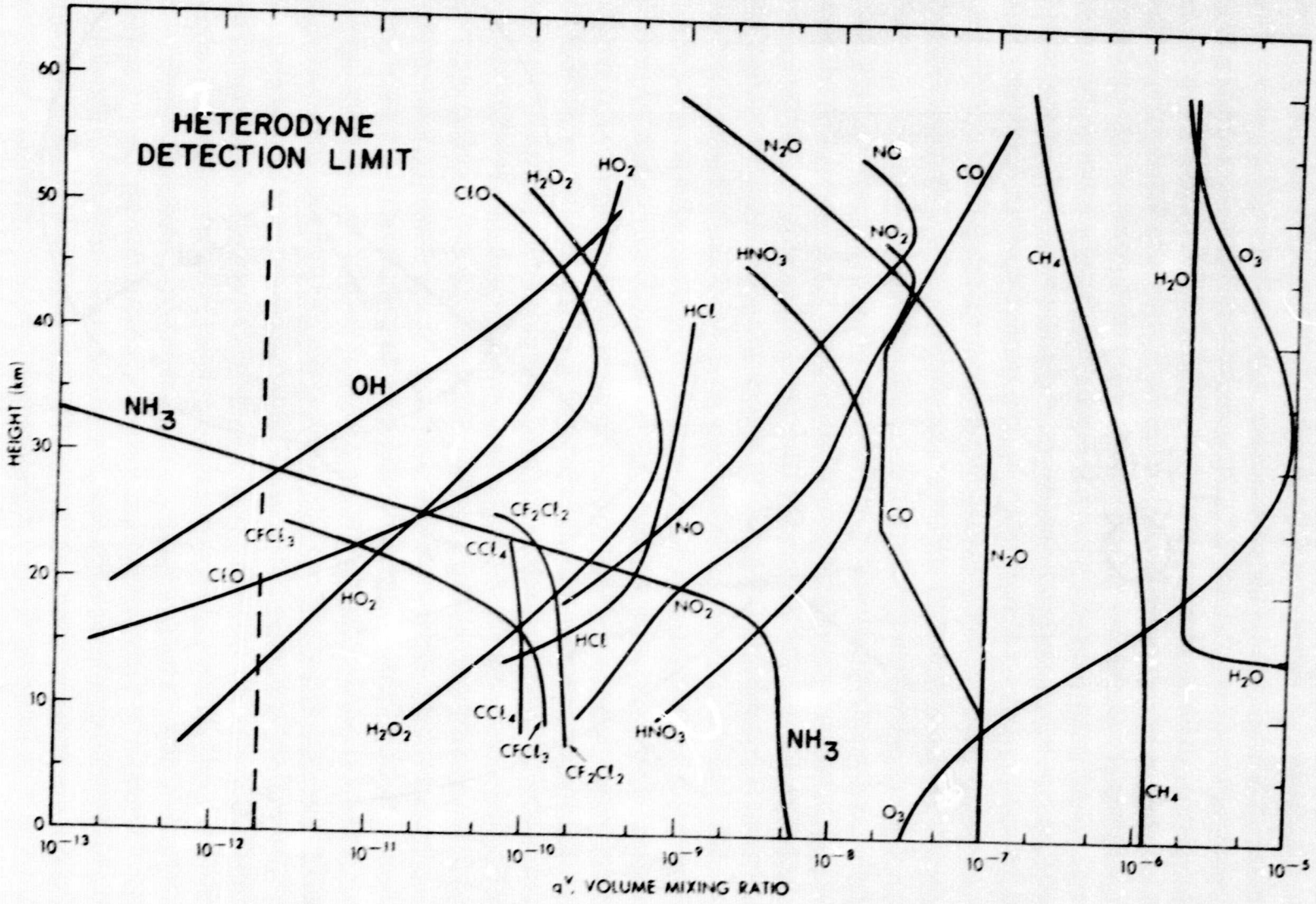
HETERODYNE
DETECTION LIMIT
HEIGHT (km)
60
50
40
30
20
10
0
NH3
OH
ClO
H2O2
HO2
N2O
NO
CO
NO2
HNO3
CH4
H2O
O3
HCl
CF2Cl2
CFCl3
CCl4
NO2
HNO3
NH3
10−13
10−12
10−11
10−10
10−9
10−8
10−7
10−6
10−5
q^v, VOLUME MIXING RATIO

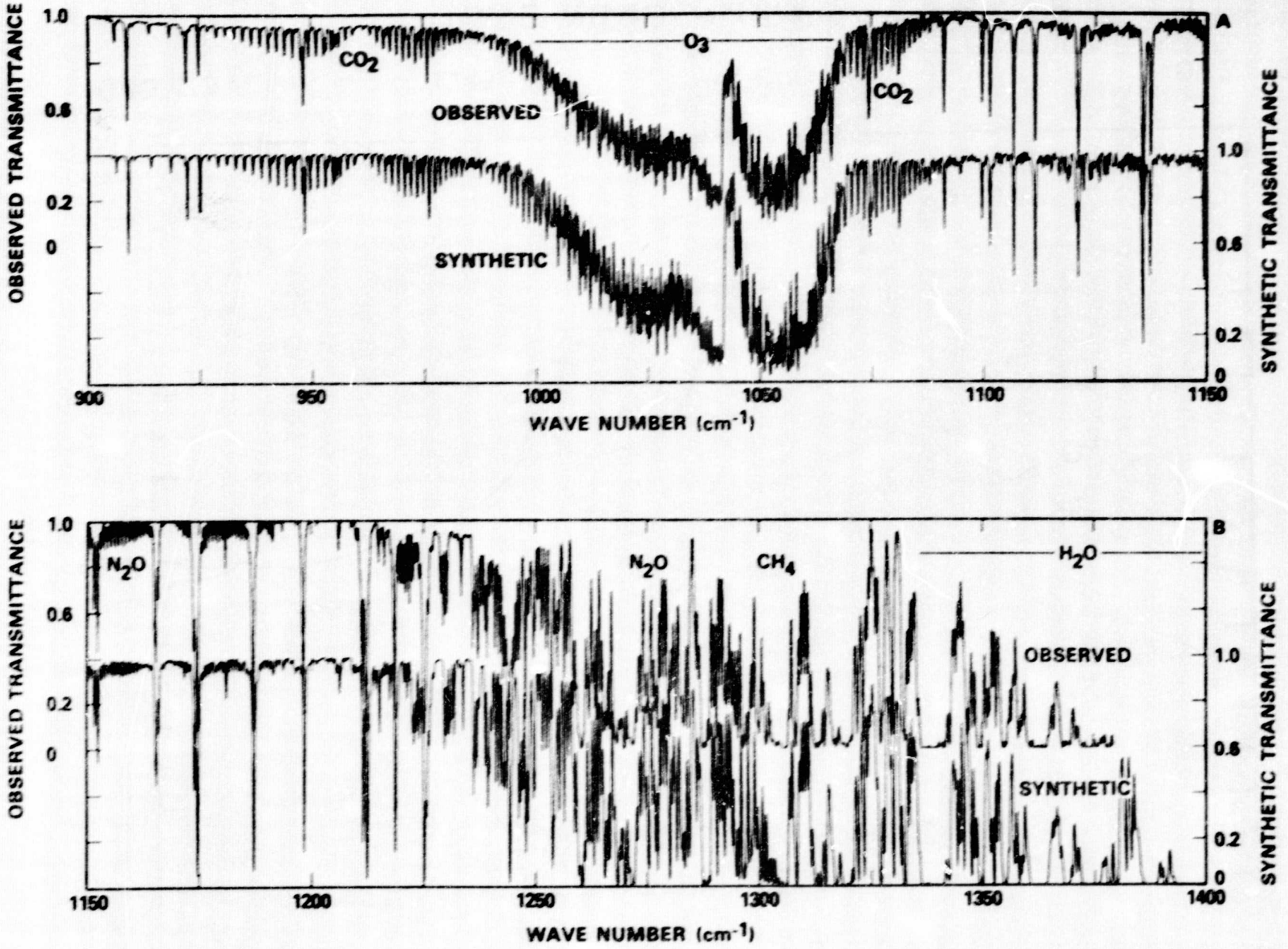
OBSERVED TRANSMITTANCE
1.0
0.6
0.2
0
CO_2
O_3
OBSERVED
SYNTHETIC
CO_2
A
1.0
0.6
0.2
0
SYNTHETIC TRANSMITTANCE
900
950
1000
1050
1100
1150
WAVE NUMBER (cm^{-1})
OBSERVED TRANSMITTANCE
1.0
0.6
0.2
0
N_2O
N_2O
CH_4
H_2O
B
OBSERVED
SYNTHETIC
1.0
0.6
0.2
0
SYNTHETIC TRANSMITTANCE
1150
1200
1250
1300
1350
1400
WAVE NUMBER (cm^{-1})

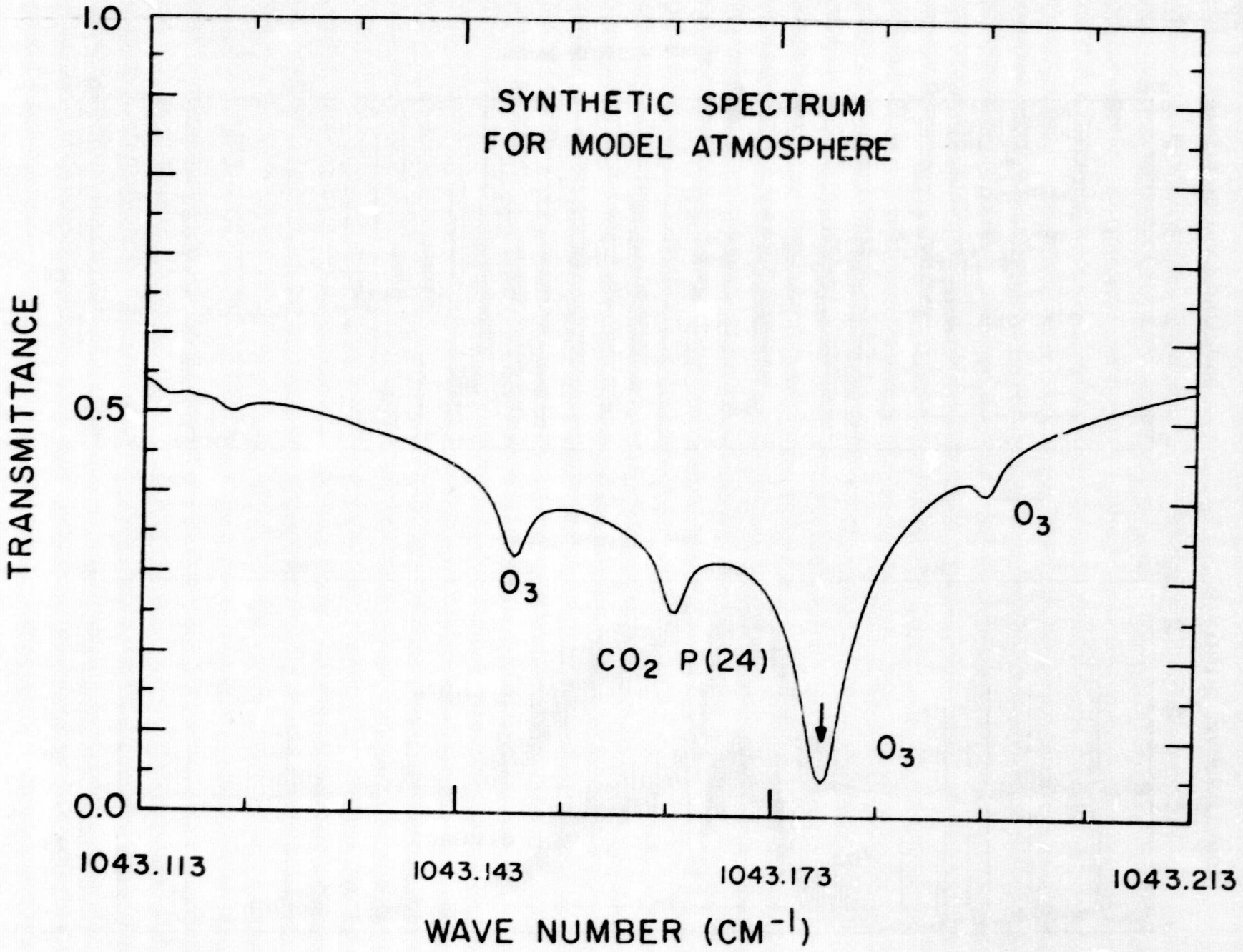
SYNTHETIC SPECTRUM
FOR MODEL ATMOSPHERE
TRANSMITTANCE
1.0
0.5
0.0
O3
CO2 P(24)
O3
O3
1043.113
1043.143
1043.173
1043.213
WAVE NUMBER (CM-1)

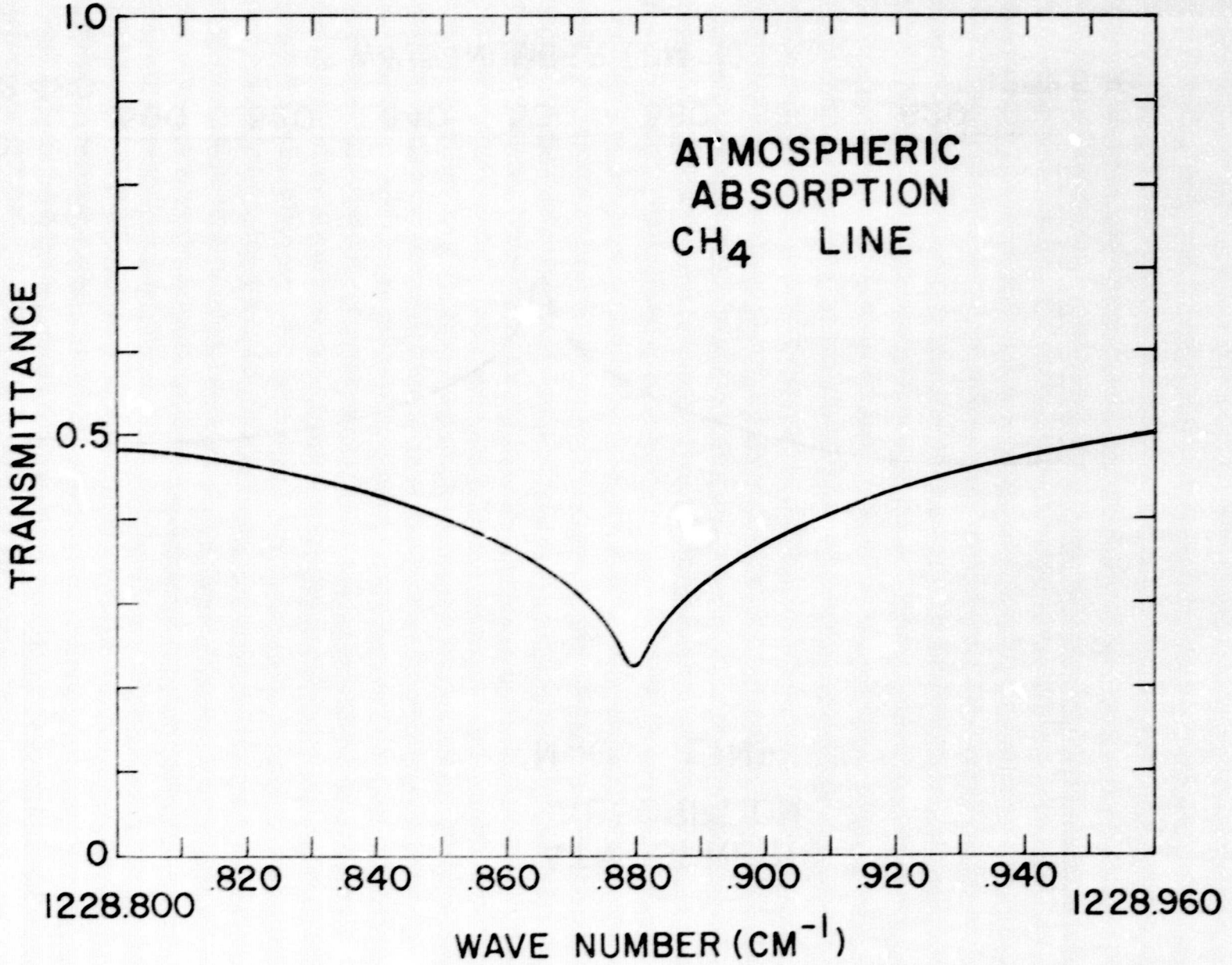
ATMOSPHERIC
ABSORPTION
CH4 LINE
TRANSMITTANCE
1.0
0.5
0
1228.800
.820
.840
.860
.880
.900
.920
.940
1228.960
WAVE NUMBER (CM-1)

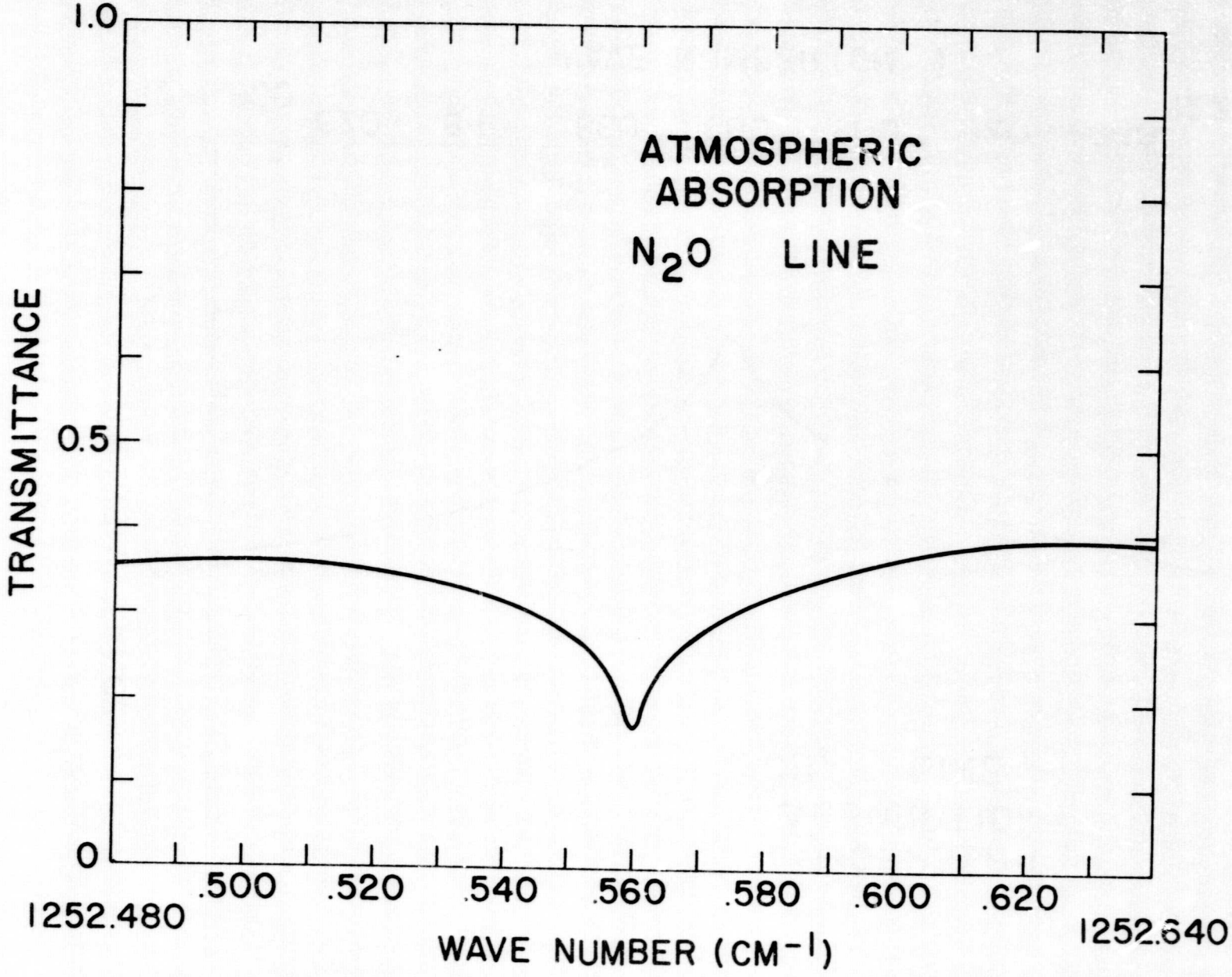
ATMOSPHERIC
ABSORPTION
N_2O LINE
TRANSMITTANCE
1.0
0.5
0
.500
.520
.540
.560
.580
.600
.620
1252.480
1252.640
WAVE NUMBER (CM^{-1})

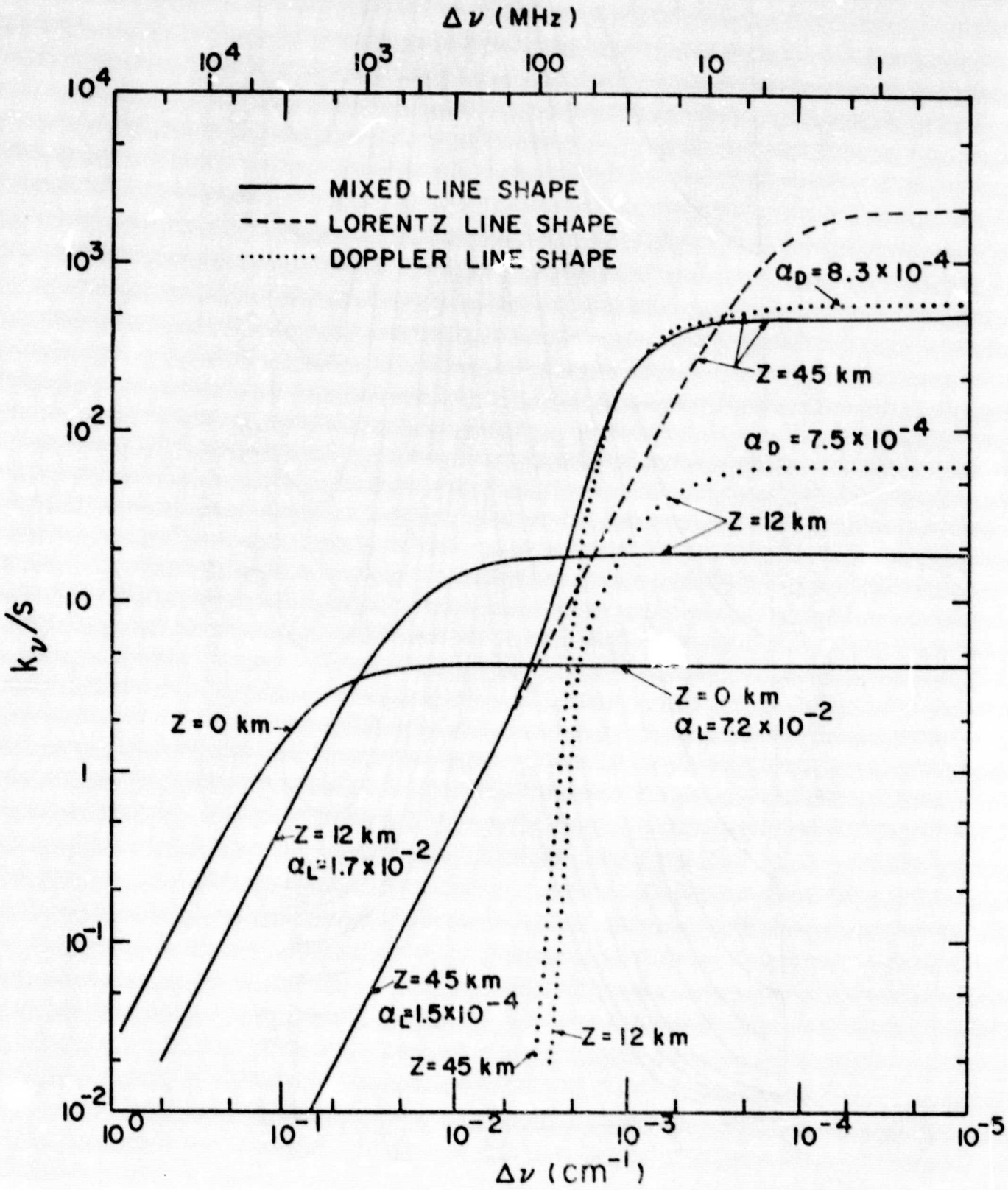
Δν (MHz)
10^4
10^3
100
10
1
MIXED LINE SHAPE
LORENTZ LINE SHAPE
DOPPLER LINE SHAPE
α_D = 8.3 x 10^-4
Z = 45 km
α_D = 7.5 x 10^-4
Z = 12 km
Z = 0 km
α_L = 7.2 x 10^-2
Z = 0 km
Z = 12 km
α_L = 1.7 x 10^-2
Z = 45 km
α_L = 1.5 x 10^-4
Z = 12 km
Z = 45 km
k_ν/s
10^4
10^3
10^2
10
1
10^-1
10^-2
10^0
10^-1
10^-2
10^-3
10^-4
10^-5
Δν (cm^-1)

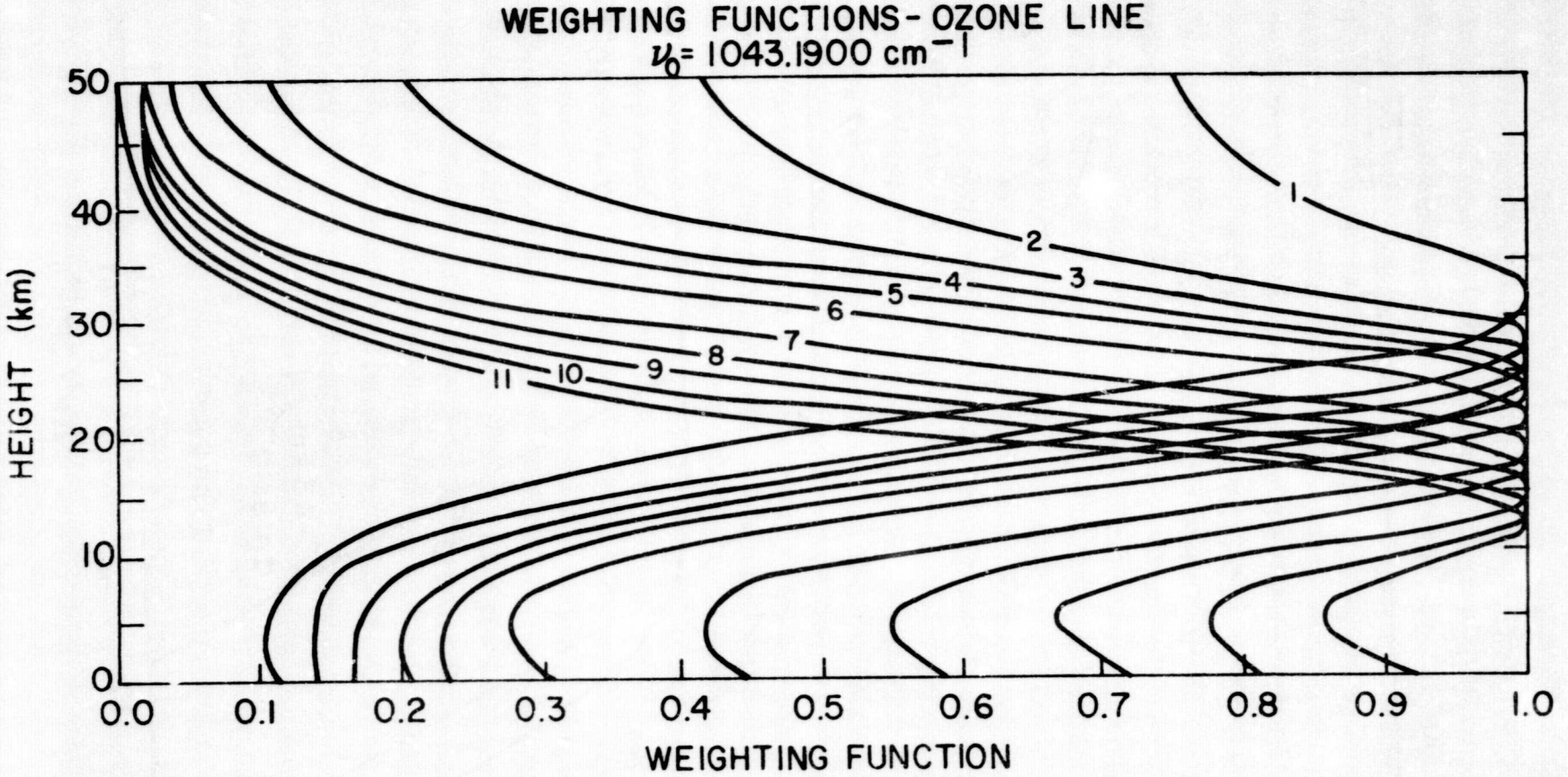
WEIGHTING FUNCTIONS - OZONE LINE
ν_0 = 1043.1900 cm^{-1}
HEIGHT (km)
50
40
30
20
10
0
0.0
0.1
0.2
0.3
0.4
0.5
0.6
0.7
0.8
0.9
1.0
WEIGHTING FUNCTION
1
2
3
4
5
6
7
8
9
10
11

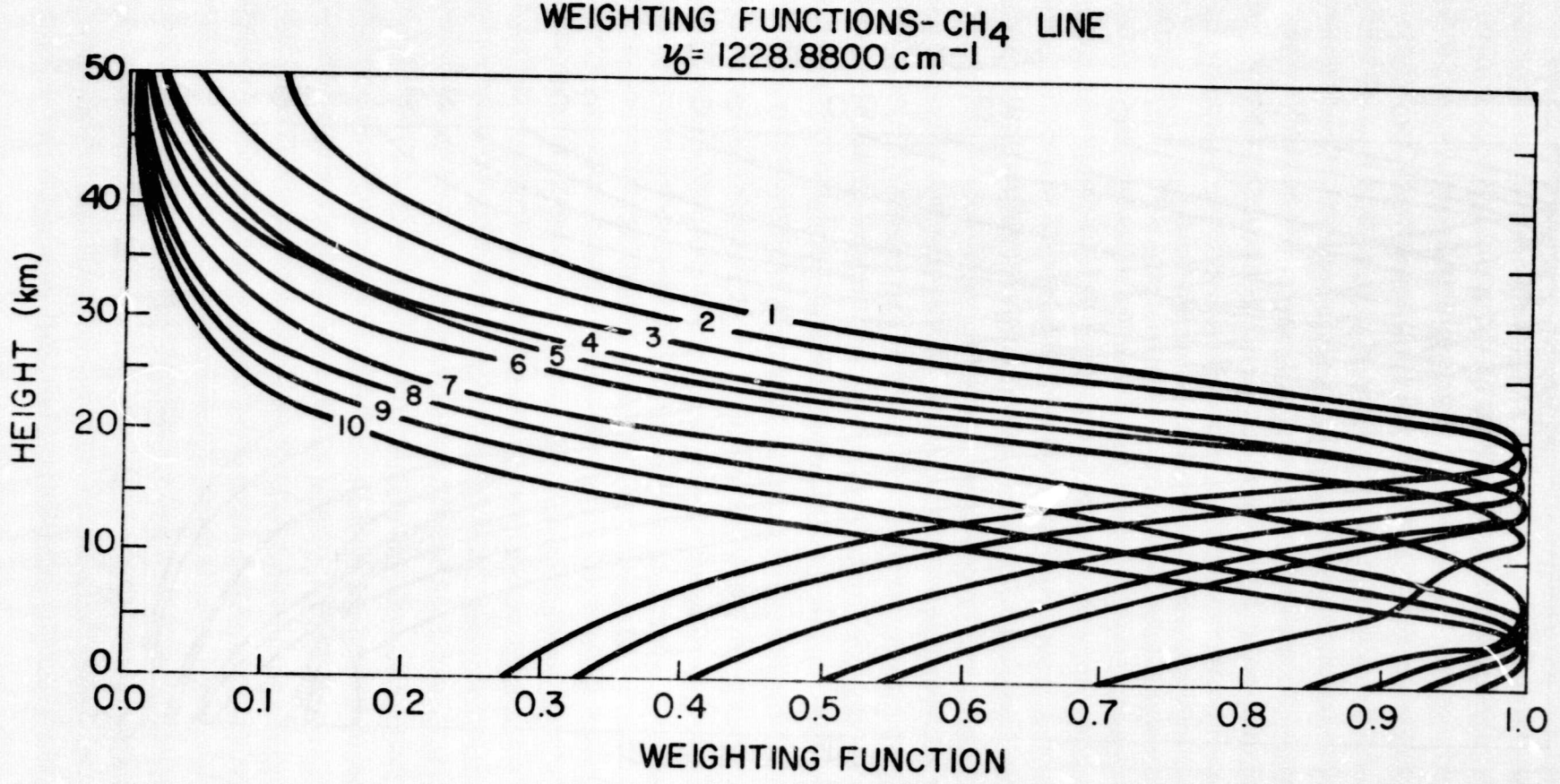
WEIGHTING FUNCTIONS- CH_4 LINE
ν_0= 1228.8800 cm^{-1}
HEIGHT (km)
50
40
30
20
10
0
0.0
0.1
0.2
0.3
0.4
0.5
0.6
0.7
0.8
0.9
1.0
WEIGHTING FUNCTION
1
2
3
4
5
6
7
8
9
10

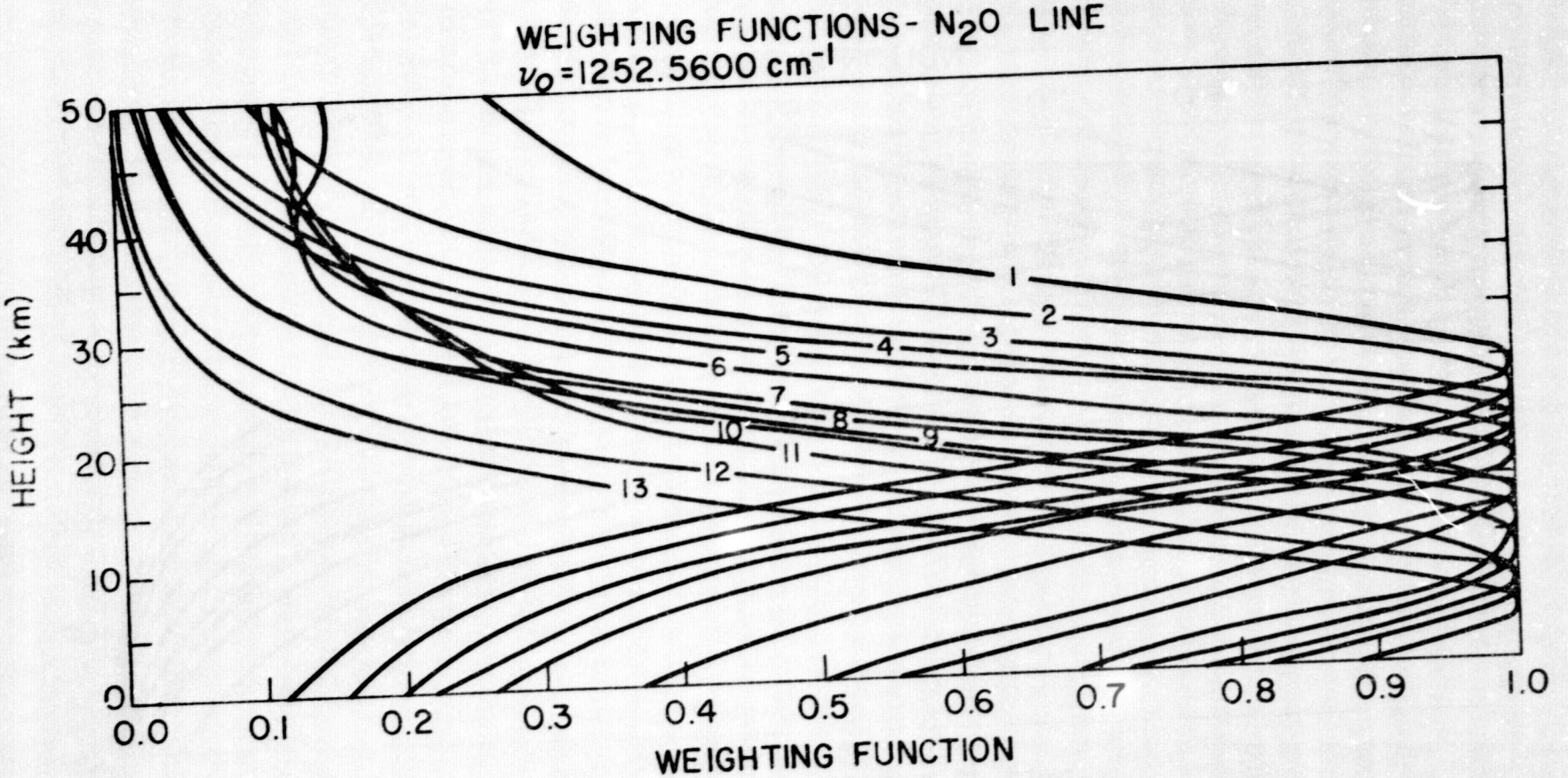
WEIGHTING FUNCTIONS- N_2O LINE
ν_0=1252.5600 cm^{-1}
HEIGHT (km)
50
40
30
20
10
0
0.0
0.1
0.2
0.3
0.4
0.5
0.6
0.7
0.8
0.9
1.0
WEIGHTING FUNCTION
1
2
3
4
5
6
7
8
9
10
11
12
13

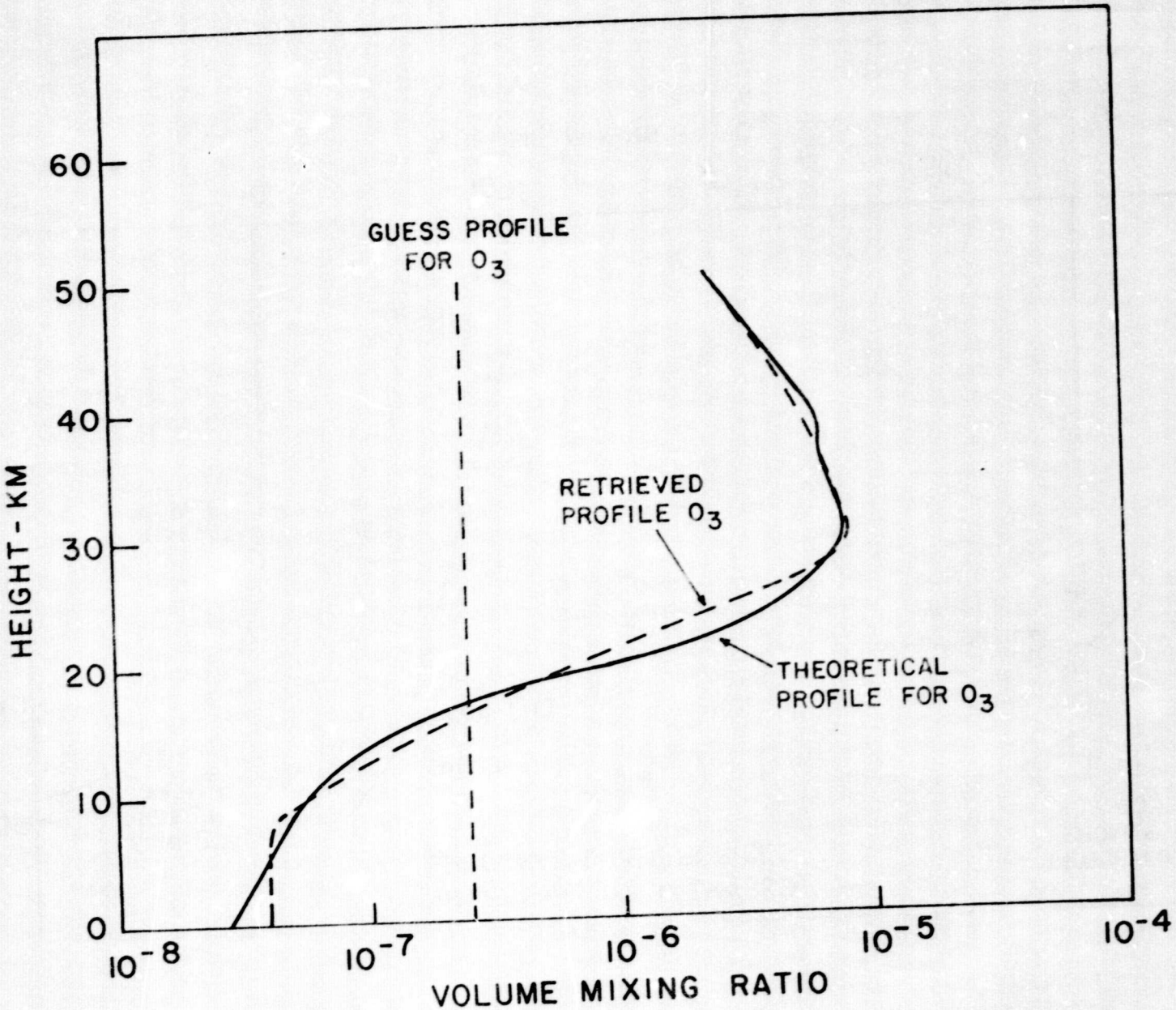
60
50
40
30
20
10
0
HEIGHT - KM
GUESS PROFILE
FOR O_3
RETRIEVED
PROFILE O_3
THEORETICAL
PROFILE FOR O_3
10^{-8}
10^{-7}
10^{-6}
10^{-5}
10^{-4}
VOLUME MIXING RATIO

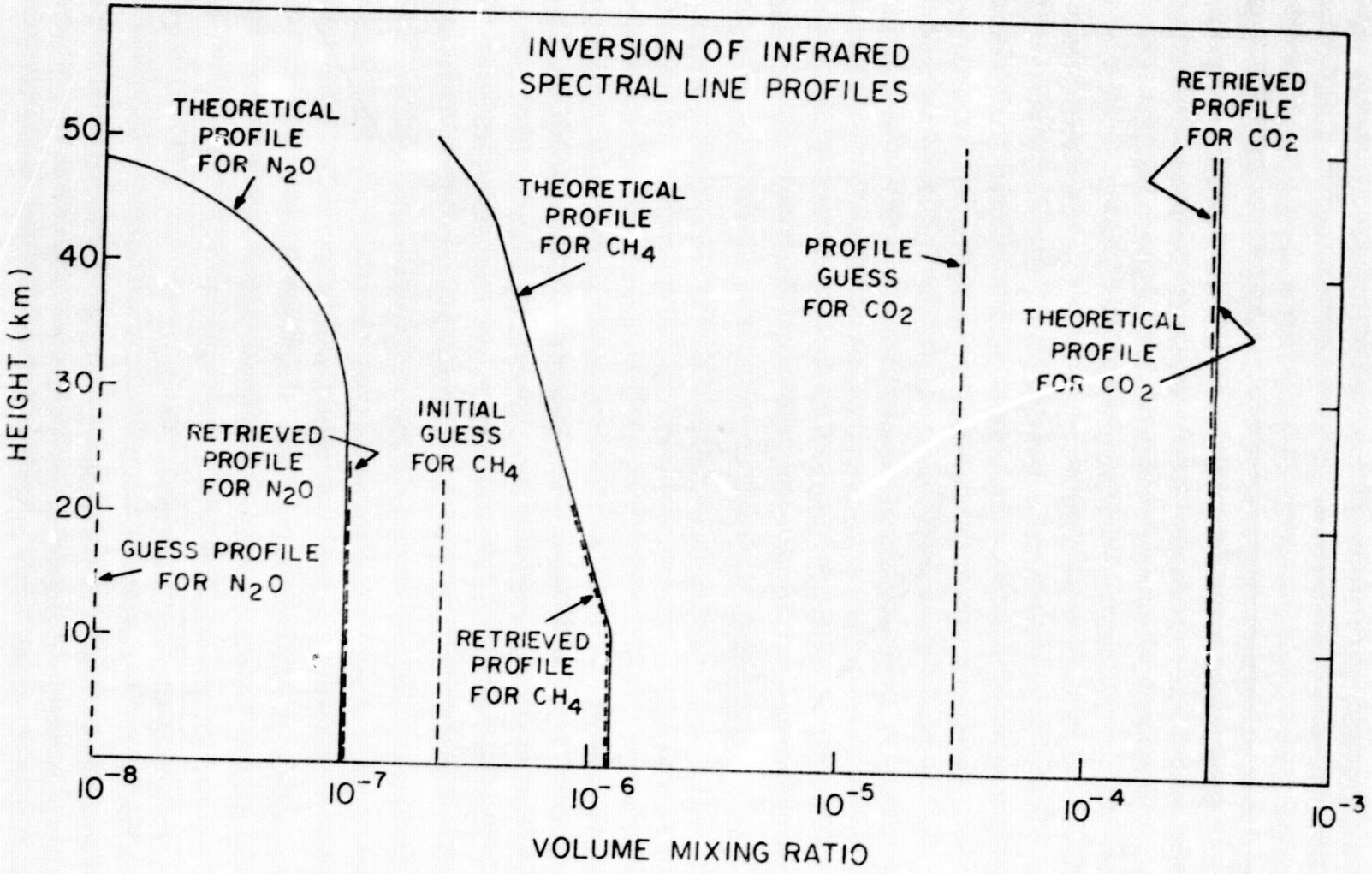
INVERSION OF INFRARED
SPECTRAL LINE PROFILES
THEORETICAL
PROFILE
FOR N_2O
THEORETICAL
PROFILE
FOR CH_4
PROFILE
GUESS
FOR CO_2
RETRIEVED
PROFILE
FOR CO_2
THEORETICAL
PROFILE
FOR CO_2
RETRIEVED
PROFILE
FOR N_2O
INITIAL
GUESS
FOR CH_4
GUESS PROFILE
FOR N_2O
RETRIEVED
PROFILE
FOR CH_4
HEIGHT (km)
50
40
30
20
10
10^{-8}
10^{-7}
10^{-6}
10^{-5}
10^{-4}
10^{-3}
VOLUME MIXING RATIO

GSFC HETERODYNE SPECTROMETER

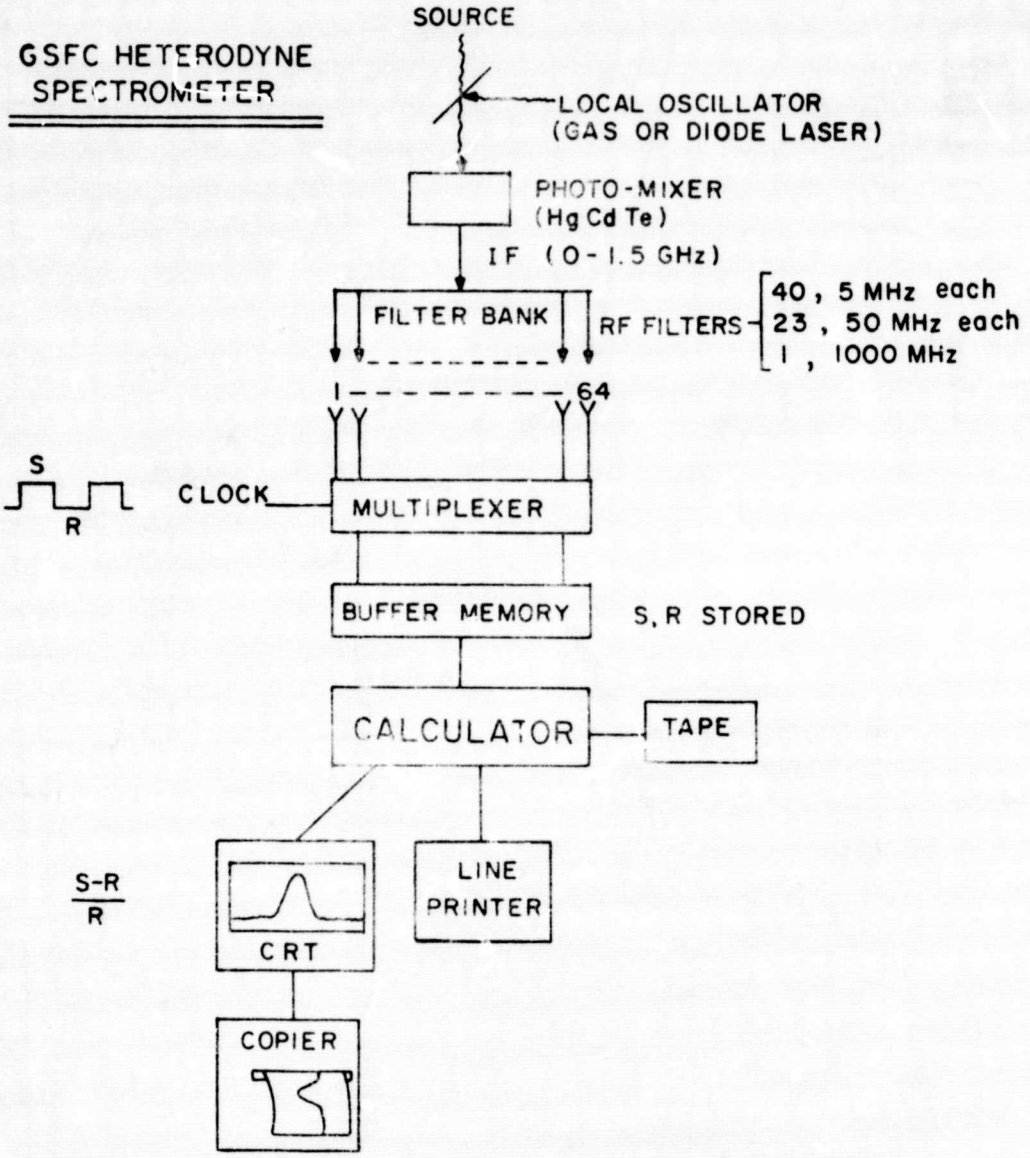

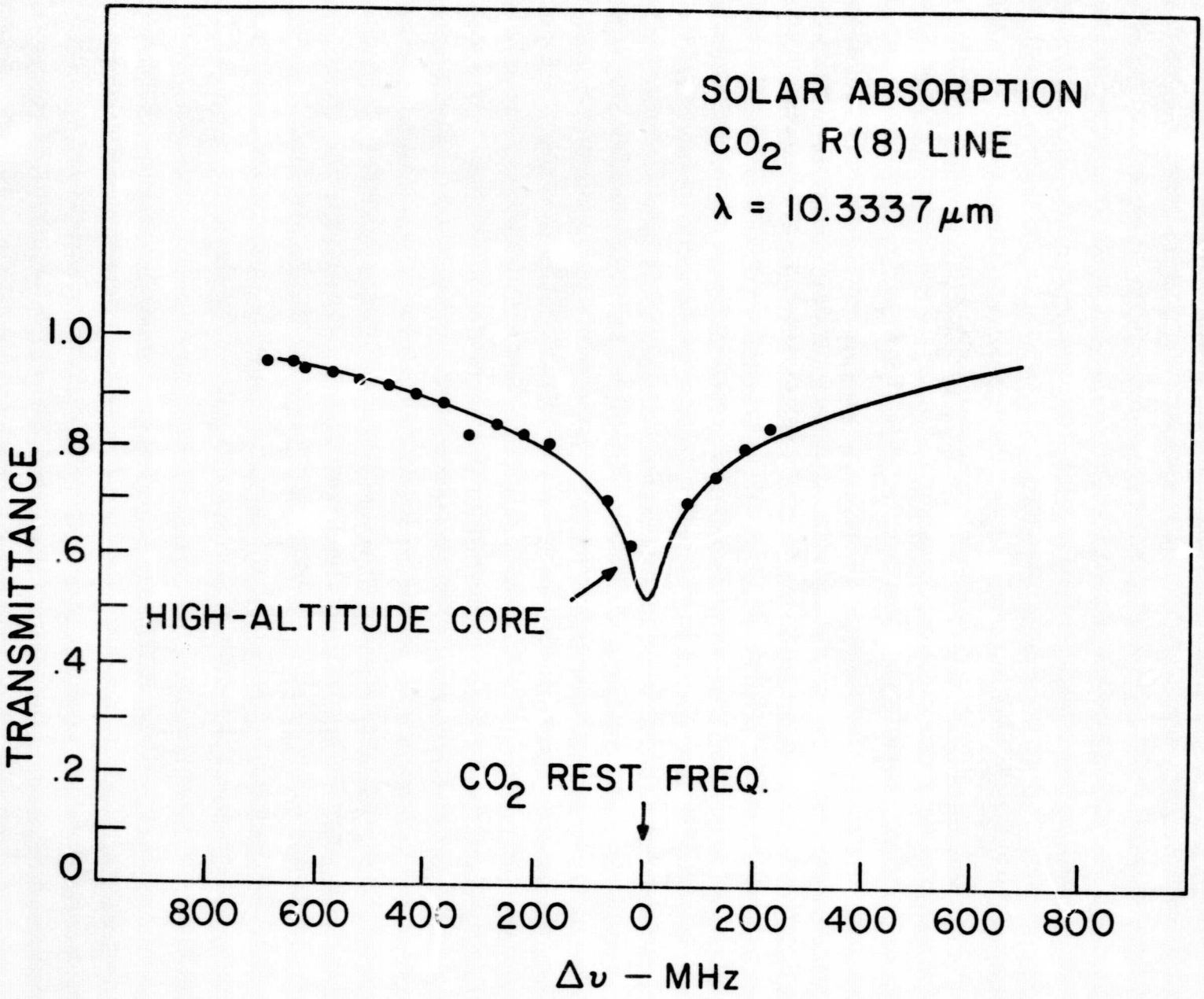
SOLAR ABSORPTION
CO_2 R(8) LINE
λ = 10.3337 μm
TRANSMITTANCE
1.0
.8
.6
.4
.2
0
HIGH-ALTITUDE CORE
CO_2 REST FREQ.
800
600
400
200
0
200
400
600
800
Δυ — MHz

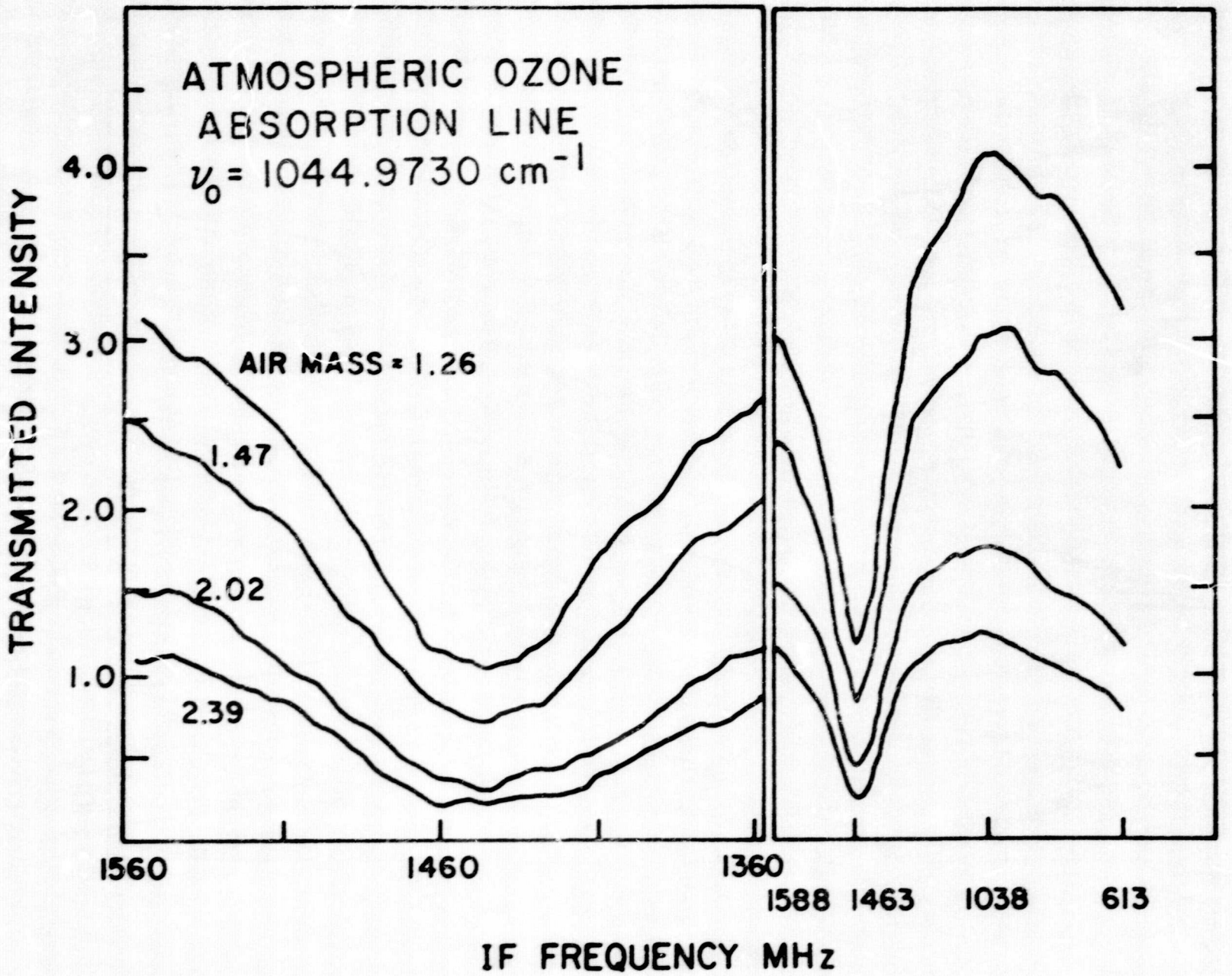
ATMOSPHERIC OZONE
ABSORPTION LINE
ν_0 = 1044.9730 cm^{-1}
AIR MASS = 1.26
1.47
2.02
2.39
TRANSMITTED INTENSITY
4.0
3.0
2.0
1.0
1560
1460
1360
1588
1463
1038
613
IF FREQUENCY MHz

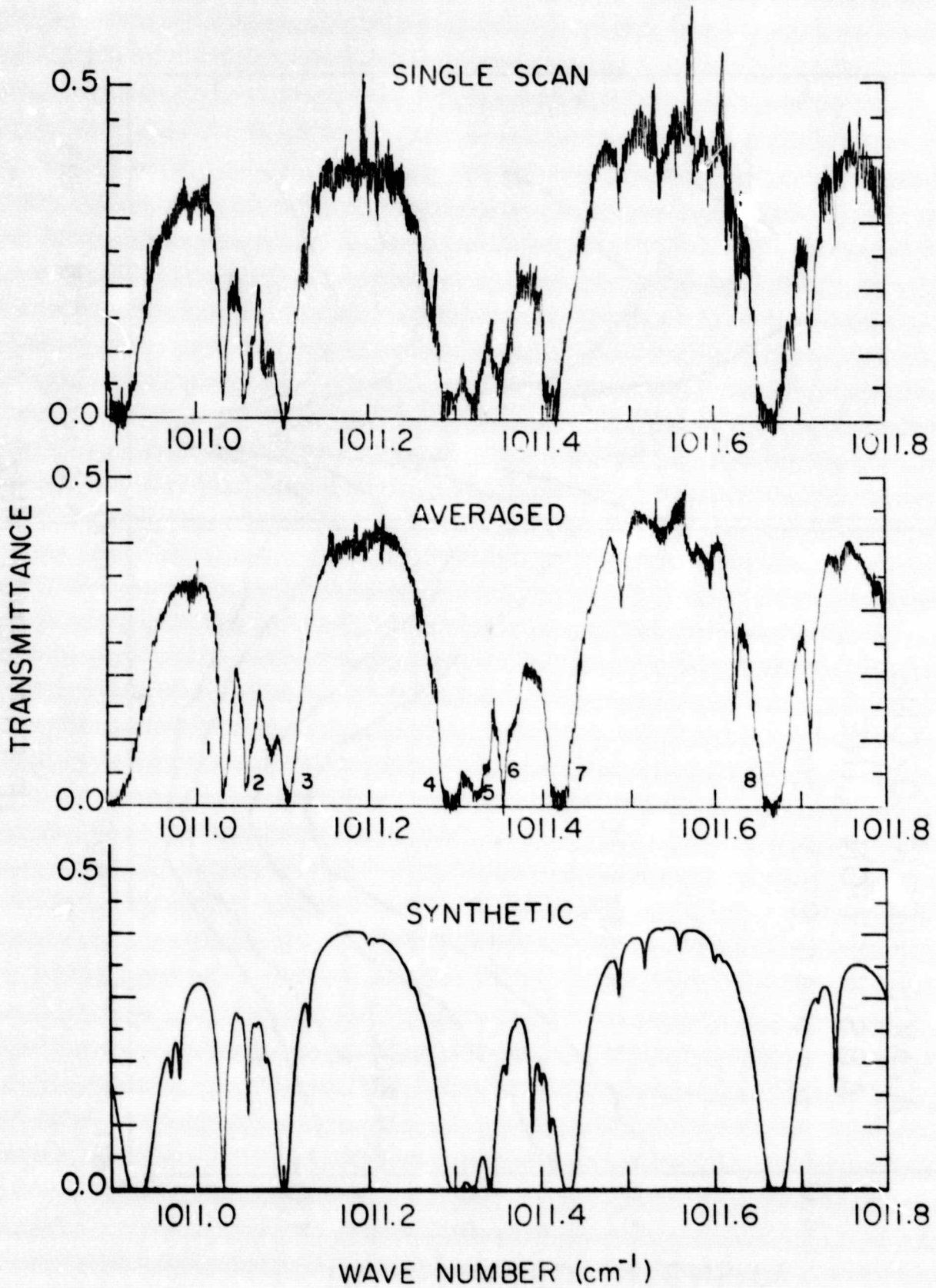
SINGLE SCAN
AVERAGED
SYNTHETIC
0.5
0.0
1011.0
1011.2
1011.4
1011.6
1011.8
1
2
3
4
5
6
7
8
TRANSMITTANCE
WAVE NUMBER (cm⁻¹)

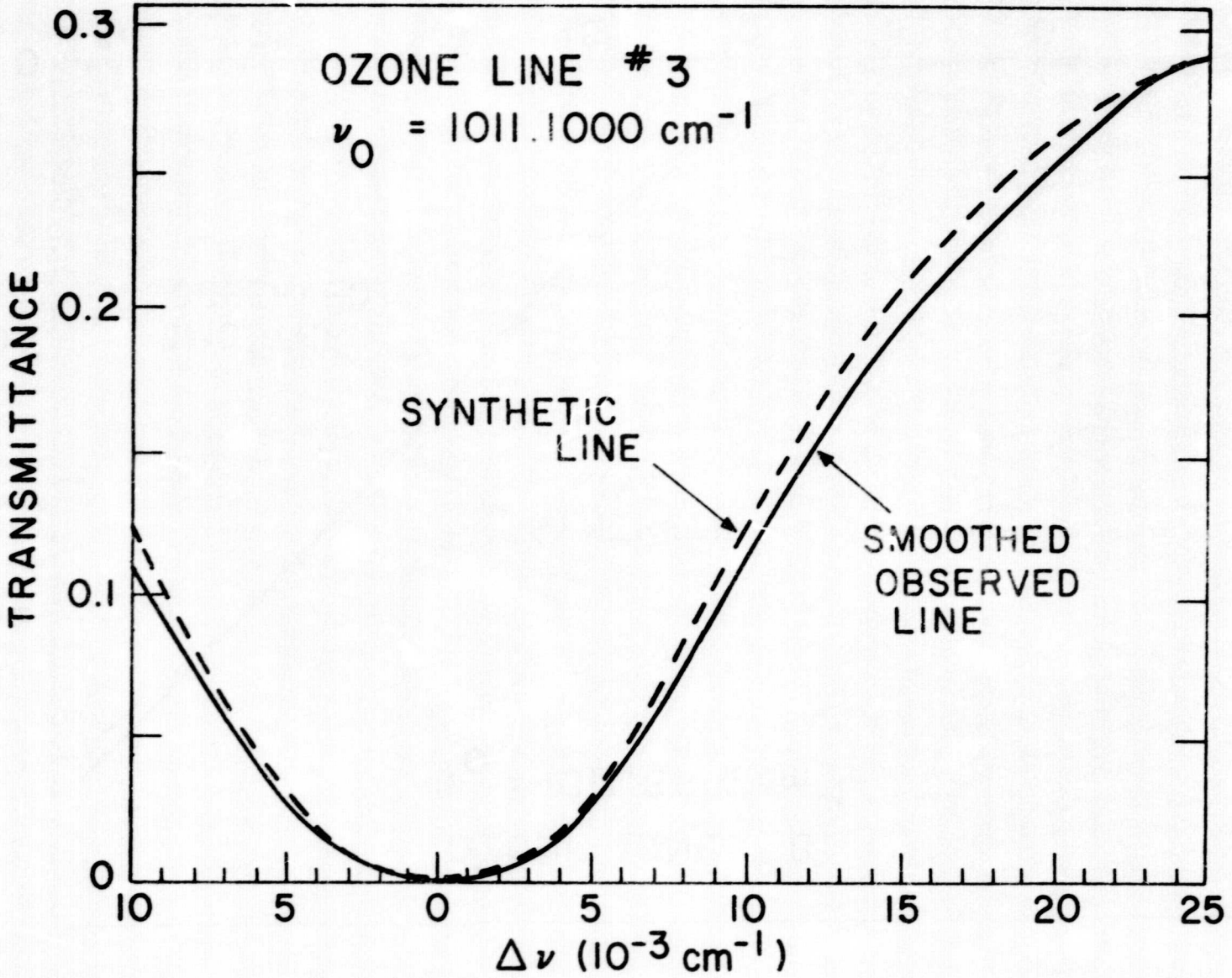
OZONE LINE # 3
ν_0 = 1011.1000 cm^{-1}
SYNTHETIC LINE
SMOOTHED OBSERVED LINE
TRANSMITTANCE
0.3
0.2
0.1
0
10
5
0
5
10
15
20
25
$\Delta\nu$ (10^{-3} cm^{-1})

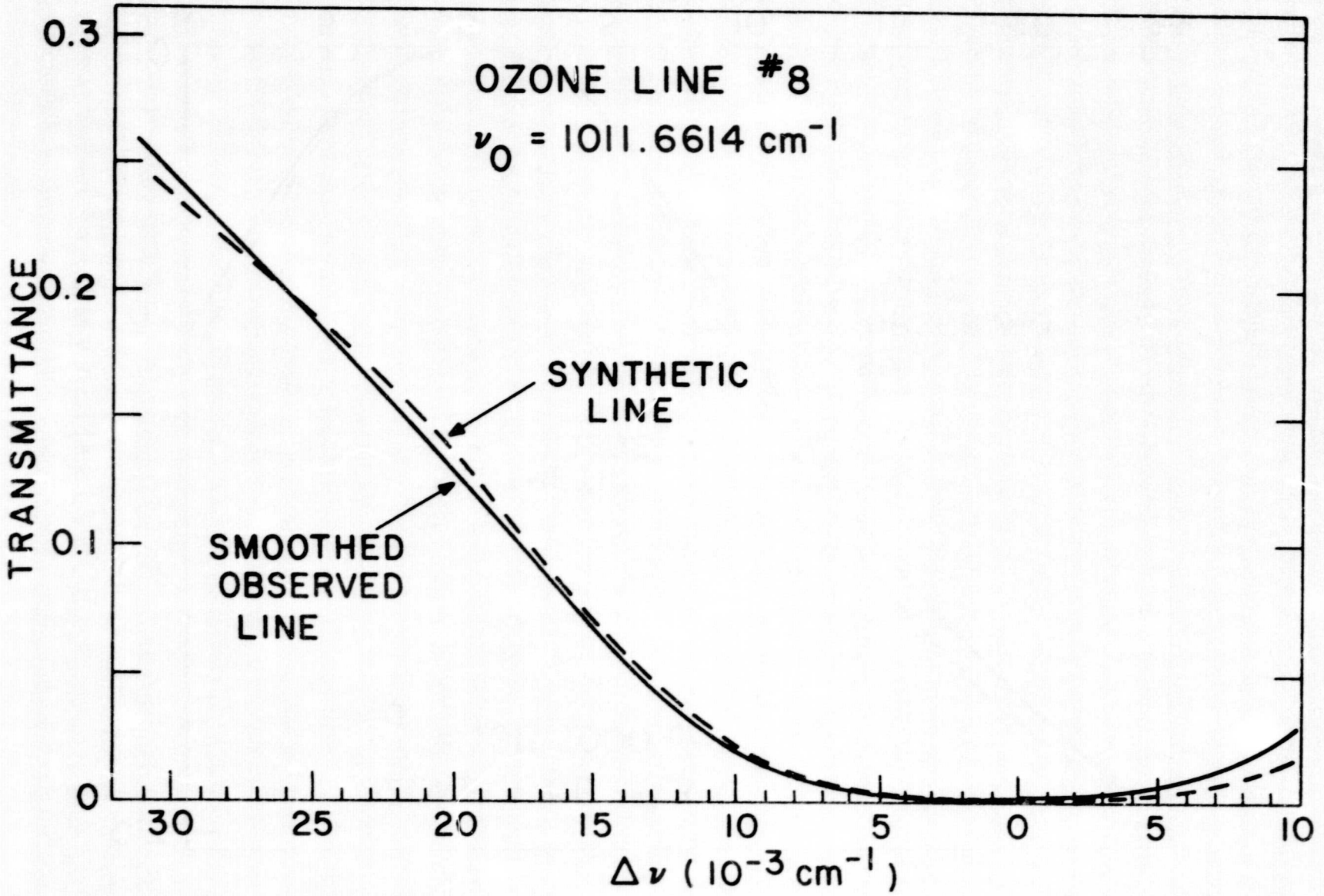
OZONE LINE #8
ν_0 = 1011.6614 cm^{-1}
SYNTHETIC LINE
SMOOTHED OBSERVED LINE
TRANSMITTANCE
0.3
0.2
0.1
0
30
25
20
15
10
5
0
5
10
$\Delta\nu$ (10^{-3} cm^{-1})

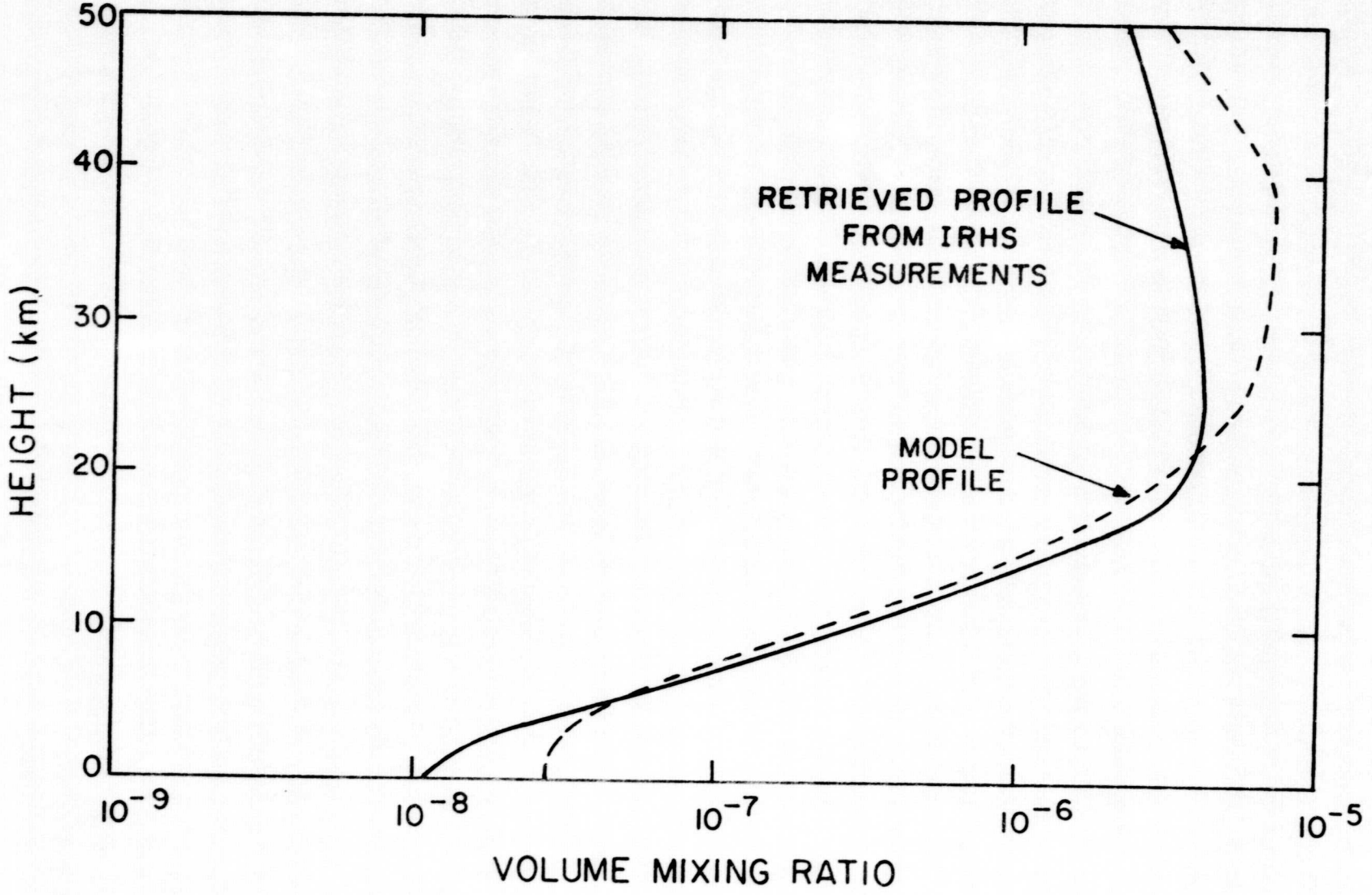
50
40
30
20
10
0
HEIGHT (km)
RETRIEVED PROFILE
FROM IRHS
MEASUREMENTS
MODEL
PROFILE
10^{-9}
10^{-8}
10^{-7}
10^{-6}
10^{-5}
VOLUME MIXING RATIO

BIBLIOGRAPHIC DATA SHEET

1. Report No.	2. Government Accession No.	3. Recipient's Catalog No.
4. Title and Subtitle Stratospheric Sounding by Infrared Heterodyne Spectroscopy		5. Report Date 6. Performing Organization Code
7. Author(s) Mian M. Abbas, Virgil G. Kunde, Michael J. Mumma, Theodor Kostiuk, David Buhl		8. Performing Organization Report No.
9. Performing Organization Name and Address		10. Work Unit No. 11. Contract or Grant No.
12. Sponsoring Agency Name and Address NASA/Goddard Space Flight Center		13. Type of Report and Period Covered 14. Sponsoring Agency Code

15. Supplementary Notes

16. Abstract Intensity profiles of infrared spectral lines of stratospheric constituents can be fully resolved with a heterodyne spectrometer of sufficiently high resolution ($\sim$ 5 MHz or 0.000167 cm^{-1}). The constituents' vertical distributions can then be evaluated accurately by analytic inversion of the measured line profiles.

Estimates of the detection sensitivity of a heterodyne receiver are given in terms of minimum detectable volume mixing ratios of stratospheric constituents, indicating a large number of minor constituents which can be studied. Stratospheric spectral line shapes, and the resolution required to measure them are discussed in light of calculated synthetic line profiles for some stratospheric molecules in a model atmosphere. The inversion technique for evaluation of gas concentration profiles is briefly described and applications to synthetic lines of O_3, CO_2, CH_4 and N_2O are given. Some recent heterodyne measurements of CO_2 and O_3 absorption lines are analytically inverted and the vertical distributions of the two gases are determined.

17. Key Words (Selected by Author(s))	18. Distribution Statement		
19. Security Classif. (of this report)	20. Security Classif. (of this page)	21. No. of Pages	22. Price*

*For sale by the National Technical Information Service, Springfield, Virginia 22151.